SPATIAL DIVERSITY GAINS IN WIRELESS SENSOR NETWORKS THROUGH CONTROLLED LIMITED MOBILITY: AN EXPERIMENTAL APPROACH

A Thesis

Submitted to the Graduate School
of the University of Notre Dame
in Partial Fulfillment of the Requirements
for the Degree of

Master of Science in Electrical Engineering

by

Matthew Brennan, Bachelor of Science in Electrical Engineering

---

Martin Haenggi, Director

Graduate Program in Electrical Engineering
Notre Dame, Indiana
May 2007

SPATIAL DIVERSITY GAINS IN WIRELESS SENSOR NETWORKS THROUGH CONTROLLED LIMITED MOBILITY: AN EXPERIMENTAL APPROACH

Abstract

by

Matthew Brennan

While Wireless Sensor Networks (WSNs) are a rapidly growing field, they still face many challenges. Some of these issues such as critical nodes, small-scale fading, and hidden nodes can be mitigated through the application of controlled limited mobile (COLMO) systems. Small movements on the scale of a fraction of the carrier wavelength can prove to dramatically change the received signal strength (RSS) and thus, link quality. With the proper sampling, it is possible to place a mobile node in a position with favorable multipath fading and greatly increase the link quality. This ability could have huge ramifications on the network, and new routing paths are enabled; therefore, new metrics and trade-offs need to be considered.

By placing a Mica mote on a rotating turntable, the mote has the ability to control the location the platform so that the mote can be placed where desired. The performance of the mobile sink was analyzed in environments with various forms of fading to determine how the diversity gain of this system compares to a MIMO design.

Several factors affecting the performance of the mobile sink were explored. One important issue is whether the received signal strength indicator (RSSI) or

the link quality indicator (LQI) would be the most effect link quality metric. Also, the thesis determines how the sampling rate of the sampled channel affects the general performance of the mobile node.

CONTENTS

FIGURES

TABLES

CHAPTER 1

WIRELESS SENSOR NETWORKS

1.1 General Overview

The field of wireless sensor networks (WSN) provides many amazing opportunities along with numerous unique challenges. WSNs are groups of individually powered powered sensor nodes that are designed to sense an aspect of their immediate environment and then transmit their acquired information to a basestation that processes this information and reacts accordingly [27]. There are many variations to this concept depending on the what needs to be accomplished. The number of sensors could range from several sensor nodes to several hundred thousand. With so many individual sensor nodes present in the system, it would be cost-prohibitive and labor-intensive to replace the energy supply for each and every node. Also, it is highly unlikely that every one of the sensors will have a one-hop connection to the basestation of the network. Since WSNs have such a wide range of possible layouts and issues, it requires its own unique architecture and standards [47], [25].

The rest of Chapter 1 will continue with the overview of the WSN. It will cover the various challenges and applications that are present and then end with an overview of some hardware platforms popular for research and general use.

Chapter 2 will cover in greater detail the actual physical environment surrounding the motes and how issues such as fading can be assessed and surmounted. Since

Ricean fading and, in particular, Rayleigh fading, are prevalent between motes in a WSN, a small amount of mobility may allow the motes to move into a position with less severe fading.

In Chapter 3, we will analyze the application of a sink with limited mobility and how it may solve various problems that plague WSNs such as unbalanced energy usage among motes in the network. In environments with intense amounts of fading, even nodes relatively close to the sink may be lacking a one-hop connection and must use valuable bandwidth by taking multiple hops to reach to the sink. The application of a mobile sink can solve this issue.

We will cover link metrics in and techniques for measuring the link quality between two motes Chapter 4. Since mobility consumes energy which is usually considered extremely precious in WSN, it is desired to keep the movements to a minimum and to position the mote in the most ideal position, the one with the highest link quality. There are several ways of measuring link quality, and this chapter analyzes the costs and benefits of each.

The final chapter, Chapter 5, will show how the performance of the controlled limited mobile (COLMO) system can be improved with the adjustment of the distance between samples. We will also demonstrate the effectiveness of several interpolation techniques that are useful when the channel is not severely oversampled spatially such that the distance between the samples are weakly correlated, but we need to know the information between the sampled positions.

1.2 Applications

The potential applications for WSNs are legion with opportunities ranging from the medical field to the military battlefield. Each situation has its own

requirements and subsequent challenges that reinforces the need for a diverse range of capabilities from the WSN field. This diversity allows WSNs to reach out from electrical engineering and be applied in other various fields such as biology and civil engineering.

One proposed use for WSNs is to monitor the structural health of buildings, bridges, or roads [19]. These structures can undergo various forms of stress and dilapidation that may not be easy to detect and correct until the problem becomes catastrophic. By then, it may prove more economical to replace the structure rather than fixing it. A solution to avoiding this scenario would be to apply a WSN by placing various sensors throughout key regions of the structure. These sensors would detect vital signs such as excess strain, tearing, or abnormal vibrations. Once any of the sensors detect something alarming, it would relay the information to a basestation that would then carry out the appropriate response. This allows the people monitoring the structure to better understand the level of damage or severity of decay throughout the building.

WSNs can also prove vital for biology experiments as demonstrated in a floral monitoring project in Hawaii in [3]. Here, the WSNs were designed to monitor the growth and activity of different endangered plants through the application of various sensors and a high-resolution cameras. After making the desired measurements, the motes monitoring the plants relayed the pictures and data from the temperature, humidity, rainfall, and wind sensors to a gateway connected to the Internet several miles away. Once the data was uploaded, the team could process the data and make detailed observations. An added challenge was that the motes had to be camouflaged to prevent detection from uninvolved by passers such as hikers that may pick up the mote due to its novelty in that environment.

Some monitoring applications can have more direct lifesaving possibilities with one example given in [9]. Here, a WSN can be used to help emergency and hospital workers save lives by assisting the emergency workers to locate and rescue victims and determine the level and promptness of care that each victim needs. This resource management could become vital in the case of a disaster arising from events such as earthquakes or terrorist attacks. In these cases, the emergency workers may become swamped and find their usefulness dangerously decreased. A properly designed WSN would be able to convey to the workers the vital information that they need for maximum effectiveness.

Not all WSN applications are peaceful since the number of military applications is about just as boundless. One such example is the research into creating a self-healing minefield. A popular and old tactic for a counteracting a minefield was to clear out a narrow path through it. As long as the path remained marked, the rest of the mines were useless in deterring the trespassers. The WSN solution to this problem is create a self-healing minefield. The sensors on the mines would detect that several mines have been destroyed by the attackers clearing a path. The network reacts by moving some mines in the network into the space that had been previously cleared out and thus increase the overall effectiveness of the mines. So far, the only way to counteract a self healing minefield using a WSN is to clear a very wide path instead, and this will effectively slow down the attackers [1].

Another military application is to use a WSN to localize a sniper once he fires his rifle. While this ability would prove extremely useful in urban combat, it is also very difficult to do with conventional means due to the acoustic multipath cased by buildings and the difficulty of acquiring a line of sight (LOS). However,

WSNs may be able to surmount these problems. In the experiment done in [2], the sensors listened for the sound and then placed a timestamp. Next, they sent the information to a basestation (BS) that would process this data and determine the location of the sniper.

There are also abundant examples of commercial applications for WSNs such as the case of using WSNs in vineyards in [4]. WSNs can ease and improve the management of sensitive agriculture crops such as grapes for wine. It can be used to automate certain systems such as irrigation control when more water is needed, or even have the grapes sprayed when one of the motes detects mildew on the plants. Another interesting concept was the application of data mules to transport the information from the motes in the field to a BS much farther away. Sometimes it was impossible for a mote or a cluster of motes to directly send information to the BS. Motes were attached to the tools such as shovels used by the workers in the fields to serve as relays. The workers would take the tools with the attached motes to the fields in the morning, and the motes would store the data from the motes in the fields. When the workers returned the tools later that day, the motes on the tools would convey all the data they collected to the BS.

1.3 Challenges

Just like the possible applications for the WSNs, the number of challenges for this system is staggering. Since the WSN is still a relatively new field, many ideas and models are still being shared and debated. Since some of these models are more correct than others, many of the problems are still not well understood. This in turn leads to making it even more challenging in finding the proper solution for the problems ranging from the physical layer to the routing layer.

Many WSNs would be applied in environments difficult for wireless communications such tropical jungles, densely crowded offices, or disaster sites. One of the metrics for measuring the efficiency of a WSN is to determine the connectivity of the network by counting the ratio of sensor and relay nodes able to reach the BS to the number of nodes that are isolated. In most situations, an isolated node is considered wasted. Usually these nodes are on the edges of the network or isolated due to its surrounding geographic features and lack of available relays.

The first and foremost issue with WSNs is energy usage. Nearly all proposed solutions and system must have this problem in consideration. While computational power has been able to adhere to Moore's Law for the last few decades, battery efficiency has doubled only every 35 years [30]. This problem is further compounded by the fact that most sensor motes in WSNs must be as small as possible. For example, many motes that can be bought off the shelf such as most of the Mica and Telos motes use two AA batteries while some motes are even smaller. Additionally, the mote's batteries cannot be replaced in many situations. Since some WSNs will use up to thousands of motes in environments that are difficult to reach, it would be expensive and labor-prohibitive to be constantly replacing the batteries on the motes.

This can severely limit the capabilities of the sensor motes on several different levels. For example, certain types of coding processes are energy-prohibitive due to the amount of computational power that they demand. Also, the demand to lower transmission power only serves to exacerbate the low SNR issue between two sensor motes. However, it has been surmised that raising the transmission power may have a lower effect on power drainage when compared to the added benefits of a higher SNR [15].

The energy concern also demonstrates the necessity of sleep modes and other practical energy saving techniques. In sleep mode, most of the functions on the mote are shut down, and the device periodically uses some energy to listen for a wake up request from another mote. In some cases, the current usage drops to 7% of the awake mode [35]. This can significantly extend the lifetime of the mote in the network. The mote is unable to transmit or collect data while it is asleep so the MAC and routing protocols must put this in consideration when the sleep mode application is applied.

Other techniques have shown to decrease the energy usage such as dynamic modulation scaling in [8]. This paper proposes that the relay mote should use the largest constellation that the channel will allow, which grants the mote the opportunity to save energy with lower radio duty cycles.

Another major problem that plagues WSNs is the rapid energy drainage of critical nodes. The goal of sensor motes in WSN is detect and relay the result to the BS, but as the relayed data is closer to the BS, less and less routes become available since fewer motes are present to relay the data. This means that the nodes surrounding the BS will have to relay far more packets to the BS than the motes farther away [33]. This scenario is displayed in Figure 1.1. Here, nodes 4 and 8 have to relay the majority of the traffic due to their proximity to the BS. Therefore, they could be transmitting three times more traffic than nodes farther away from the BS. These critical motes vital to the WSN are also losing their battery energy the most quickly. Eventually, the critical nodes will lose all their energy while the sensor nodes farther away will remain fresh. Once this happens, the WSN will greatly lose its effectiveness.

A desired quality in WSN models is the ability to scale since many applications

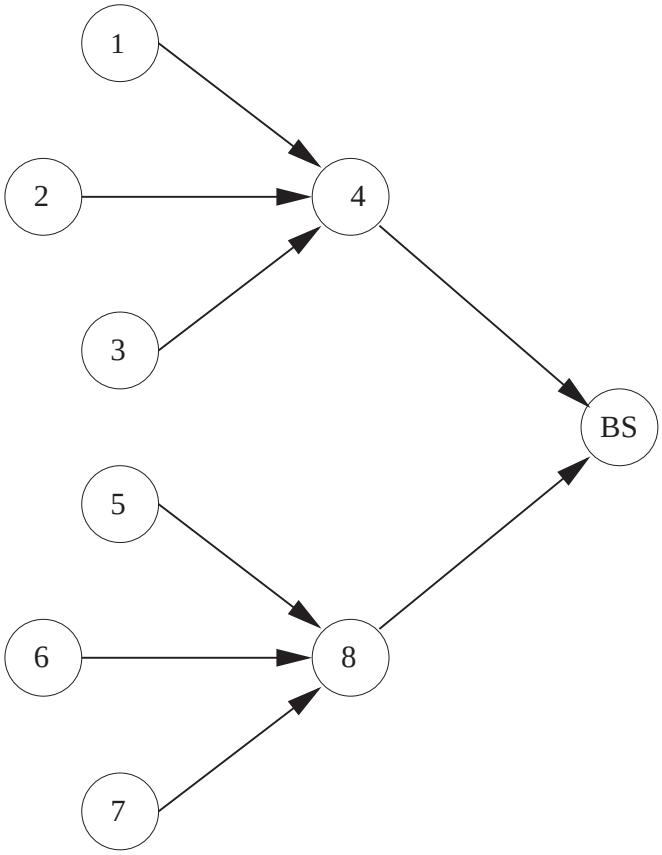

Figure 1.1. Nodes 4 and 8 are the critical nodes since they must relay all the packets sent to the BS.

can easily require several thousand motes. As the network becomes larger, more relays are going to be needed to relay the info from the sensor mote to the BS. Dropped packets penalize the WSN with extra latency and wasted energy since more power will be needed to retransmit the message. Also, the large number of retransmissions leads to a larger response time for the overall WSN.

Adjustments to the MAC layer can be done to help reduce power drainage by improving the throughput and efficiency of the WSN. A MAC protocol designed for large scale WSNs is better able to reduce the number of energy wasting collisions and control packet overhead.

1.4 Routing Metrics

Routing is a key issue in the overall performance of a WSN. A routing protocol designed for WSNs needs to avoid retransmissions, ensure a satisfactory throughput, and avoid issues such as premature deaths of critical nodes. Also, the work [21] has shown that changing the layer protocol to allow layer crossing between the physical layer, MAC layer, and routing layer can improve the efficiency of the WSN. Another important factor in routing is the WSN lifetime; therefore, energy-aware routing takes priority over energy-efficient routing. Energy-efficient routing protocols utilize paths that consume the least amount of energy. However, if these paths are overused, the energy of the relay nodes in that path will become rapidly depleted those causing the path and perhaps the whole network to fail as shown in [32]. Energy-aware routing, however, may use less efficient paths, but the nodes in the paths used will have more energy.

A routing protocol designed for WSNs proposed in [16] is called LEACH or Low-Energy Adaptive Clustering Hierarchy. The premise for this routing protocol

is that groups of relay nodes in proximity to each other form clusters. The nodes in each cluster are then assigned a schedule of when they will be become cluster heads with their time being randomly chosen. This helps to ensure that each node in the cluster gets nearly equal energy drainage. This can dramatically increase the lifetime of the WSN since the issue critical nodes is avoided until all the nodes start to die. Also, this protocol delegates the relay responsibilities among redundant nodes. Some nodes in the WSN may be deployed closely together which allows them to share their stored energy for the same job.

Due to the properties of some WSNs routing tables may not always be necessary or even desired. One leading alternative is Ad Hoc On demand Distance Vectoring or AODV [24]. When the source desires to convey its information to the sink, it sends out a broadcast that the relays convey to the sink. This may result in a multitude of possible paths between the source and sink. Then the most ideal path is chosen depending on the routing metric being applied. This metric is more adaptive than the routing protocols that require an established routing table.

A popular routing metric among WSNs is to use the expected number of transmissions (ETX) as the routing metric [6]. While a minimum-hop routing technique would appear practical for wired networks, the variance in link qualities must be considered in ad-hoc networks and especially in WSNs. The ETX routing metric finds and utilizes the path between the source and sink with the best link quality. It is not an energy-aware routing metric since the same path will be repeatedly used if its superior link quality remains constant, but it is very energy-efficient since it avoids as much retransmissions as possible.

Many other routing metrics and protocols exist with some being more practical and useful than others with the min-hop protocol as an example. Also, some

protocols may be limited to certain standards such as Zigbee in [23]. There are also protocols such as in [36] that apply adaptive routing to conserve energy.

1.5 Popular WSN Platforms

A popular choice for research in WSNs has been the Berkeley motes detailed in [17]. These motes from Crossbow have several designs adhering to different frequency ranges and standards. Their two more common models are the Mica2 and the MicaZ. The Mica2 is an older model that can be adjusted to have a carrier frequency of 433MHz or 868MHz. Its transceiver is the Chipcon 1000 which applies FSK modulation, and it operates with a bandwidth of 30kHz and is capable of delivering data at a rate of 76.8kbps. It also has a noise floor of -110dBm and can have a transmission power ranging from 10dBm to -20dBm. It also uses an Atmel ATmega128L which is a low-power microcontroller. Almost all the Berkeley motes are programmed with TinyOS, which is a memory-efficient operating system that can handle multiple events at once. This is critical for a WSN that may have to sense data and relay packets almost simultaneously. While this microcontroller is not nearly as powerful as a normal computer, the Mica2 only needs 2 AA batteries to properly function. A variation of the Mica2 mote is the MicaDot which has all the same qualities of the normal Mica2 but is only 2.5cm long.

A more recently released Berkeley mote is the MicaZ. One of the differences that the MicaZ has with its predecessor is that it has a Chipcon 2420 transceiver. This transceiver adheres to the IEEE 802.15.4 WPAN standard by using the Zigbee specification and uses DSSS with a spreading gain of 9dB [28]. The transceiver uses OQPSK modulation, and the carrier frequency is 2.4GHz that

transmits information at a rate of 250kbps. It has a noise floor of -94dBm and transmit power range of 0dBm to -24dBm. Like the Mica2, the MicaZ can also measure the received signal strength (RSS) of an incoming signal, but the MicaZ in addition has the ability to measure the link quality indicator (LQI) [27].

Another mote similar to the MicaZ is the moteiv Tmote Sky. It is also Zigbee compliant and utilizes the Chipcon 2420 transceiver. The noticeable difference is that it uses a USB port to interact with the computer while the Mica family have a 51 pin connector that be connected to the computer's serial port via an MIB gateway.

1.6 Contributions of the Thesis

This thesis suggests analyzes a new technique that can enhance the effectiveness of future WSNs. The application of controlled limited mobility can greatly improve the link quality between two nodes by utilizing spatial diversity. This thesis explores and details search methods that best utilize the spatial channel available to the mobile mote and compare its performance to the conventional MIMO system.

The COLMO system explored in this thesis can solve some of the WSN challenges detailed in this chapter. It shows that a BS with controlled limited mobility can have access to many nodes that are hidden from a stationary BS. This can prove useful in solving the networking issues arising from critical nodes and limited path options for routing.

Finally, we explore how the spatial variation of the channel analyzed by a node with controlled limited mobility can be interpreted. The effectiveness of the COLMO system depends greatly on the distance between samples. This thesis

details how to find an acceptable sampling rate as to further improve the performance of the COLMO system.

CHAPTER 2

SIGNAL STRENGTH ENHANCEMENT VIA SPATIAL DIVERSITY

2.1 Fading

Fading has proven to be one of the largest obstacles in wireless communications. Fading is responsible for many factors that will prevent wireless transmissions that are not a concern in wired communications.

Large-scale fading results from the shadowing caused by large obstructions such as buildings. These obstacles simply block out one or more paths between the source and sink of the signal. The magnitude of the shadowing can sometimes be correlated with the distance between the transmitter and receiver, and the shadowing can result in a large deviation from the mean of the signal strength if the obstacle is large enough to block most of the signal. Usually, the effects of the shadowing can vary by movements orders of magnitude larger than the wavelength of the carrier frequency. Therefore, the coherence length is an order of magnitude or more larger than the wavelength.

Small-scale fading can cause the received signal strength to vary greatly from the mean when the receiver or transmitter is moved by a fraction of a wavelength, and this is caused by the signal multipath propagation. The signal transmitted by the sender may bounce from several surfaces and each signal will experience differing levels of attenuation and delay. The receiver then records a superposition

of all these signals. The phase delays in the signals can lead to constructive or destructive summation.

If the multipath delay is large, there may be a large delay spread between the first and last version of the same signal. A larger delay spread results in a smaller coherence bandwidth, and if the bandwidth of the signal is larger than the coherence bandwidth, frequency-selective fading will occur. In this case, intersymbol-interference (ISI) becomes prevalent. On the other hand, flat fading occurs when the bandwidth of the signal is less than the coherence bandwidth [39]. The experiments conducted in this thesis are done under flat fading conditions.

Various other factors affect the characteristics and magnitude of the small scale fading such as the Doppler spread. If there is a larger Doppler spread such that the coherence time is less than the symbol period, the system is undergoing fast fading. If the opposite is true such that the Doppler spread is less than the baseband bandwidth due to a low Doppler spread, the system is experiencing slow fading. For the experiments and observations made in this thesis, we assume that the only slow fading since all the experiments are conducted at relatively low or no velocity.

2.2 Static Fading

We explore the application of limited, controlled mobility in an environment with static multipath fading. The signal strength and link quality are time-invariant since the obstacles in the environment are stationary. Therefore, the point-to-point signal power can be defined by:

$$y_k = a_k x_k + z_k, \tag{2.1}$$

where y_k is the received signal strength, x_k is the transmitted strength, and z_k is the additive white Gaussian noise. The variable a_k is the product of the large scale path loss and the fading coefficient as shown:

$$a_k = L\left(\|\underline{x}_T - \underline{x}_R\|\right) \cdot f(x_T, y_T, z_T, x_R, y_R, z_R). \tag{2.2}$$

L is the large-scale path loss while $f(x_T, y_T, z_T, x_R, y_R, z_R)$ is the *fading coefficient*. The large-scale path usually will not change significantly for movements a fraction of a wavelength; however, the fading coefficient can vary greatly even to movements a fraction of a wavelength. Also, the fading coefficient is generally symmetric, *i.e.*, $f(x_T, y_T, z_T, x_R, y_R, z_R)$ is nearly equivalent to $f(x_R, y_R, z_R, x_T, y_T, z_T)$.

2.2.1 Probability Distribution of the Fading Channel

The fading coefficient is deterministic although it is very difficult find the exact value for this coefficient with ray-tracing simulations since the fading is very sensitive to the properties of the surrounding environment. Nevertheless, this value can be determined through experimental measurements that can be stored and utilized in making appropriate decisions. Also, the fading coefficient can be defined and predicted via certain probability distribution models.

A transmitted signal can be broken into its in-phase and quadrature parts as in:

$$E_Z = E_R(t)\cos\left(\omega_c t + \phi_n\right) - E_I(t)\sin\left(\omega_c t + \phi_n\right), \tag{2.3}$$

where E_R is the in-phase component while E_I is the quadrature component, and they are defined as respectively:

$$E_R = E_0 \sum_{n=1}^{N} C_n \cos\left(\omega_c t + \phi_n\right), \tag{2.4}$$

$$E_I = E_0 \sum_{n=1}^{N} C_n \sin\left(\omega_c t + \phi_n\right). \tag{2.5}$$

It is assumed that E_I and E_R are independent and thus uncorrelated. Also, they must have a Gaussian distribution with zero mean. This causes the envelope to have a Rayleigh distribution. The envelope of E_Z can then be defined by Equation 2.6;

$$R = \sqrt{E_R^2 + E_Z^2} \tag{2.6}$$

This envelope represents the amplitude of the received signal, and it has a Rayleigh probability distribution:

$$p_R(r) = \begin{cases} \frac{r}{\sigma^2}\exp\left(-\frac{r^2}{2\sigma^2}\right) & \text{if } r \geq 0 \\ 0 & \text{if } r < 0 \end{cases} \tag{2.7}$$

The underlying assumption is that no LOS is present so no received signal path dominates any of the others. When a LOS exists, the signal with the LOS will dominate all the other received signals. The resulting envelope has the Ricean distribution:

$$p_R(r) = \begin{cases} \frac{r}{\sigma^2}\exp\left(-\frac{(r^2+A^2)}{2\sigma^2}\right) I_0\left(\frac{Ar}{\sigma^2}\right) & \text{if } r \geq 0 \\ 0 & \text{if } r < 0 \end{cases} \tag{2.8}$$

Here I_0 is a modified zero-order Bessel function of the first kind. As the LOS becomes weaker, the value for A starts to decrease. When A becomes zero such

that no LOS is present, the distribution is Rayleigh.

2.3 Spatial Analysis of the Fading Channel

Static multipath fading can be mitigated with the application of spatial diversity. Temporal diversity exists when the RSS varies over time. Many well known diversity methods such as repetition coding with interleaving depend of the channel being time-variant. Likewise, spatial diversity is useful when the RSS varies over a spatial region. In [29], it is shown that while there are positions with destructive fading, there are other areas where the fading enhances the RSS. This is one of fundamental premises of the MIMO systems [39], but as we will show, a mote with controlled mobility can achieve higher diversity gains than the MIMO system. A receiver with enough mobility can generate a wide range of samples while the MIMO system can take only as many samples as it has receivers.

2.4 Experimental Platform

I built a rotating platform with a motor that is controllable by either the Mica2s or MicaZs. Therefore, a Mica mote placed on the edge of the rotating platform could take samples and command the motor to rotate the platform so that the mote would be placed appropriately. In this system, the mote's distance from the center of the rotating platform remained constant so its position is defined by θ, the angle of rotation from the original position, which allows the system one degree of freedom. So if the platform rotates by π, the mote moves to the other side of the platform, and another movement by π returns the mote back to its original position. In Figure 2.1, each movement by θ would cause the mote on the perimeter of the circle to move by $\lambda/10$. Figure 2.2 shows the actual turntable

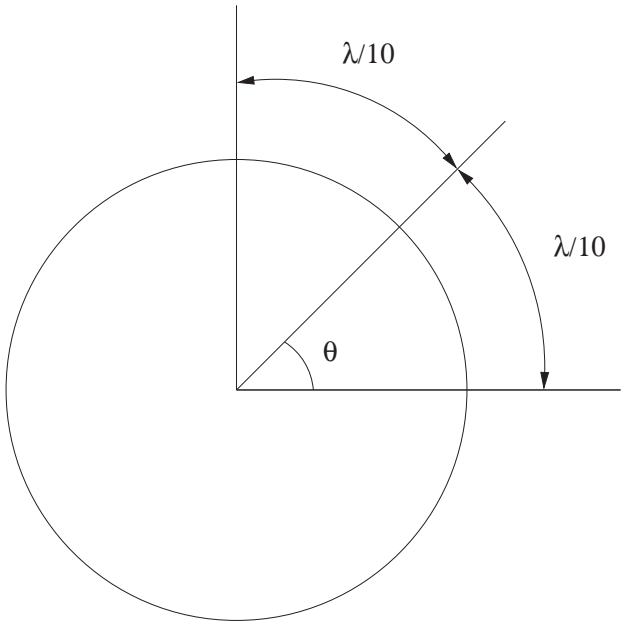

Figure 2.1. Location of the mote as a function of angle. The mote will be on the perimeter of the circle and its location is defined by the angle θ.

used in this thesis. A similar system was used in [44] where the rotating platform was used to placed the receiver into many positions with varies degrees of fading.

While the turntable mote can only analyze a periodic one-dimensional space, it still could produce enough uncorrelated samples that makes its diversity superior to the MIMO system. The function $S(\theta)$ is the signal strength of the received signal as a function of θ. In the case of the mobile receiver on the platform, θ can chosen from the continuous range $[0, 2\pi)$. MIMO systems can only take samples from a small number of antennas:

$$S(\theta_k) = f\left(\theta_0 + \frac{2\pi}{n} \cdot k\right), \quad k \in \{0, 1, \cdots, n-1\} \tag{2.9}$$

where n is the number of antennas taking samples so $2\pi/n$ is the spatial sam-

Figure 2.2. Turntable used for experiments verifying spatial diversity.

pling rate. By construction, it undersamples the spatial channel in comparison to the mobile antenna example.

The goal of the mobile antenna is not to avoid large-scale fading since that would require more energy and movement than would be practical. Instead, the goal is to use *small controlled movements* that may solve the small-scale fading issues caused by multipath. Additionally, the mobile antenna tries to use the multipath to enhance the strength of the received signal. With slight movements the size of a fraction of a wavelength that are inconsequential in the distance between the transmitter and receiver, the received signal might improve significantly.

There are many other viable options for the mobile platforms with each having their own strengths and weaknesses. For example, using a robot as a mobile platform would allow a two-dimensional sample space. This allows for a larger diversity gain in comparison to the one-dimensional sample space; however, this system can be much more complex and expensive. Of course, if the nodes are

mobile anyways, moving them to good fading spots is possible at only incremental energy costs.

2.5 Search Protocols

One of the purposes of the rotating platform is to assist the receiver in searching for the position with the strongest channel and then return to that position as closely as possible. An effective technique has been to break down this search into two stages with each using its own search protocol. The first stage utilized the Global Search, and second stage used the Local Search.

2.5.1 Global Search

The primary goal of this protocol is to make as broad of a search as possible so that all the spatial positions available to receiver are sampled and analyzed. In the case of the rotating platform, this means that the platform must do a full rotation for the receiver to complete a Global Search. While the platform is rotating, the mote takes a RSS sample at every position separated by an appropriate distance until the rotation is complete. If the distance between samples is small enough, the knowledge of the channel should be fairly useful in determining the true position with the greatest RSS. The result should appear similar to the example given in Figure 2.3.

In Figure 2.3, the continuous line represents the true signal strength of each position on the rotating platform. Each of the impulses is the sample of the signal strength taken by the receiver on the platform. If the impulses are close enough together, the receiver should have enough knowledge of the channel to determine the exact location of the maximum point. However, if the points are too far apart,

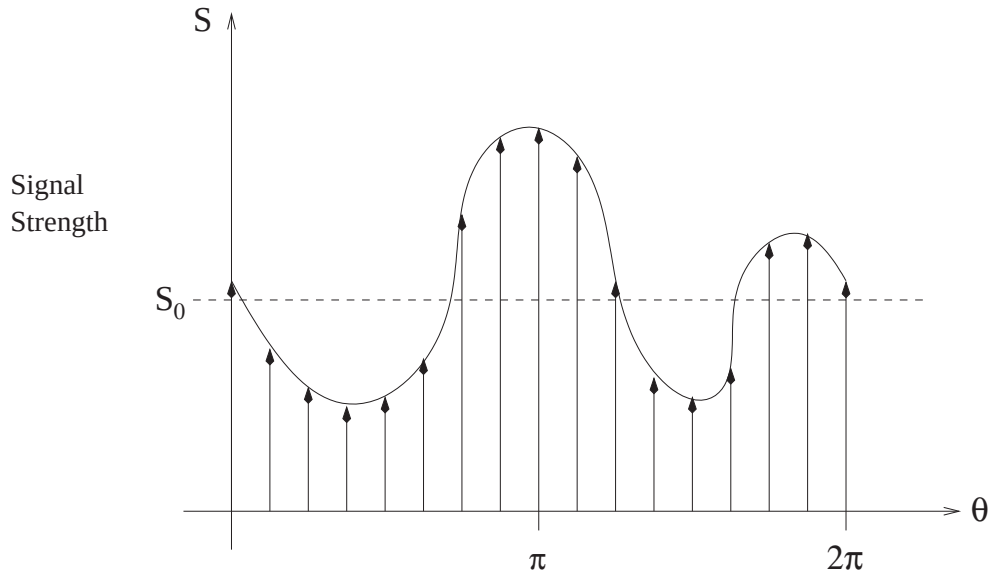

Figure 2.3. Example of a Global Search where S_0 is the mean RSS of the channel. The impulses are the actual samples taken by the mote.

then the receiver will most likely not have enough knowledge about the channel to be able to determine the ideal location.

An example of a search experiment with the Mica2 mote can be seen in Figure 2.4. Here, the channel was greatly oversampled spatially so the space between impulses is very small which makes it more simple to interpret the qualities of the spatial channel.

After the channel had been properly analyzed, the receiver returns to the location that it has determined to have the strongest signal strength. The primary goal of the Global Search is ensure that the final position is as shown:

$$\theta_{Final} = \arg\max_{\theta} S(\theta). \tag{2.10}$$

Here, the function $S(\theta)$ is the RSS for position θ. If there were more than one

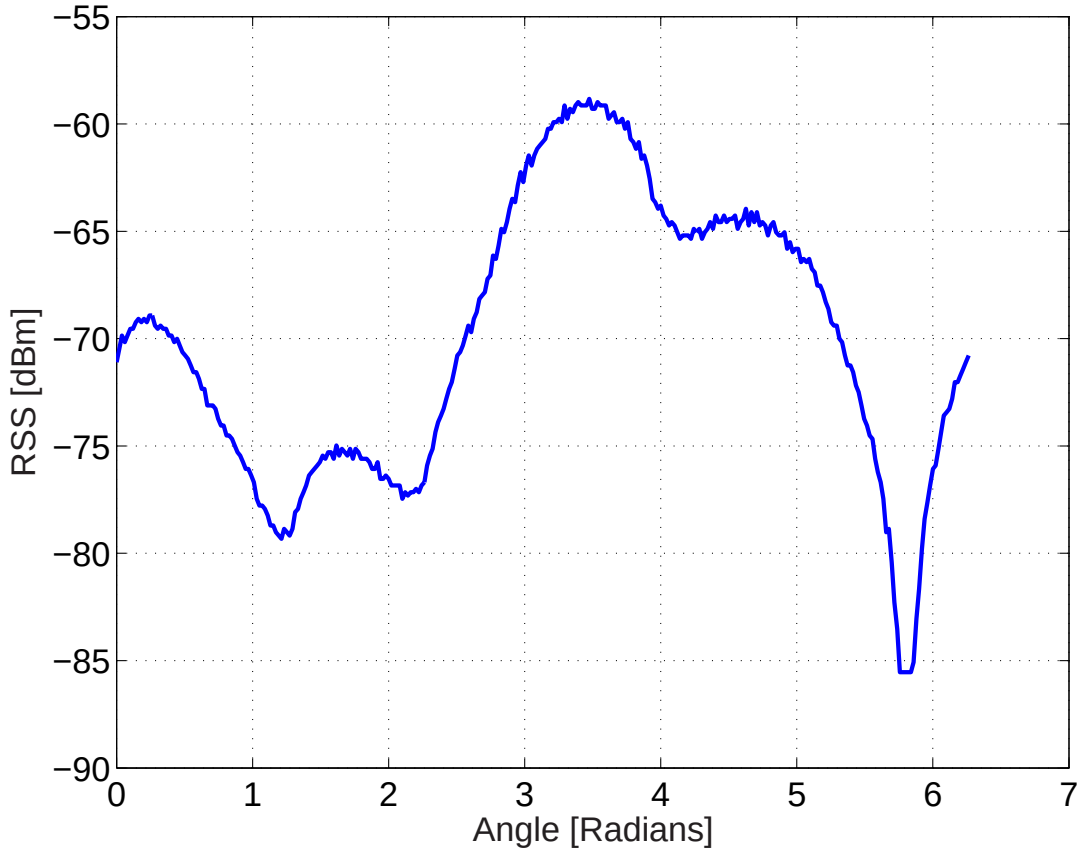

Figure 2.4. Example of the Global Search with the Mica2.

position with the largest received signal strength, the receiver would return to the position with the largest sample closest to the receivers current position at the end of the Global Search. This allows the search to be completed as quickly as possible. Physically, it is extremely unlikely that two different positions have the exact same value for the RSS. However, the mote will quantize the RSS, and two different RSS values that are relatively close to each other may be assigned the same value by the mote.

2.5.2 Local Search

The motor used for the experiments in this thesis is fairly accurate, and the Global Search alone would be sufficient in a perfect, closed system. However, due to the presence of friction, delay, platform vibrations, and other various factors, the Global Search protocol alone will unlikely perfectly return the receiver to the desired position with the highest RSS. This is a a consequence of the overall system being open loop and lacking feedback; however, most effective forms of feedback may prove too costly to apply.

The Local Search protocol is then called by the receiver to compensate for the error in positioning. The main goal of the local search protocol is to find the local maximum as shown:

$$S\left(\theta_{Final}\right) = \max\{S(\phi - \epsilon), S(\phi), S(\phi + \epsilon)\} \text{ for } \epsilon > 0. \tag{2.11}$$

If the Global Search is at least moderately effective, then the local maximum at the end of the Global Search should be the global maximum. Therefore, the Local Search will work only if the assumption that the receiver was able to return relatively close to the global maxima is valid.

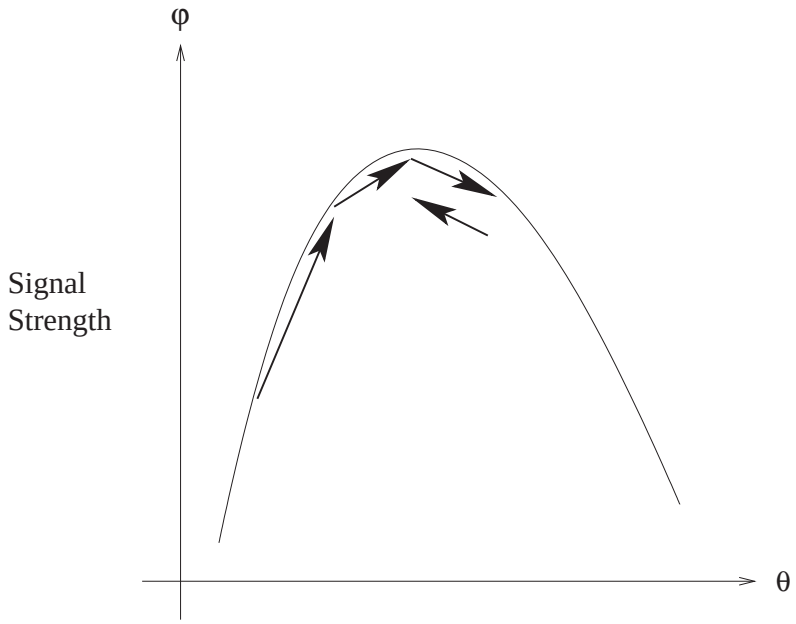

Figure 2.5. Example of the Local Search. Here, four jumps were needed to find the position with max signal strength.

The Local Search protocol starts by taking the RSS of its current position, and then it moves forward or clockwise for the case of the rotating platform. The receiver then takes another sample of the RSS while in its new spatial position. If the second RSS sample proves to be higher than the first, the platform will move forward once again and take another RSS sample. This process will continue until the new RSS sample is found to be lower than the previous sample. In this case, the platform will move backwards, or counterclockwise for the rotating platform, back to the position with the highest RSS. This is demonstrated in Figure 2.5. On the other hand, if the second sample proves to be smaller than the first sample taken in the Local Search, the platform will conduct the rest of the Local Search in reverse, or counterclockwise, in contrast to the original example.

One issue is the step size of each sample taken in the Local Search, If the step

sizes are too small, several undesired consequences may arise. At best, it may take a large amount of time for the Local Search protocol to find the ideal position since it will have to take so many samples. At worst, the samples might be taken so close to each other that they may be too correlated for the Local Search to be effective. The receiver will not be able to tell the difference between the two positions and then inaccurately assume that it has found the local maximum. However, if the spacing between samples is too large, it is possible that the receiver will overshoot, find the wrong local maximum, and miss the global maximum entirely. Therefore, the ideal step size should be small enough so that there is some correlation between samples but not too small so that the adjacent samples are too correlated.

For these experiments, it was found that $\lambda/16$ was a good sampling interval. In this case, the samples were close and correlated enough that overshooting and finding the wrong local maximum was unlikely. However, the samples were distant and uncorrelated enough that the receiver was able to tell the difference in RSS between samples.

The Local Search can be used independently from the Global Search. If the Global Search will consume too much energy to be practical, the Local Search alone may be a viable option since it requires less movement. It may not find the global maximum, but it will yield some diversity gain in the COLMO system by finding the local maximum. It can also be used in a hybrid system such that the Local Search protocol remains active even after the Global Search and a previous Local Search have been conducted. In this scenario, the Local Search will be used again in the event that the link quality drops below an established threshold. This will allow the COLMO system to remain as a practical option even in a dynamic environment where the fading is time-variant.

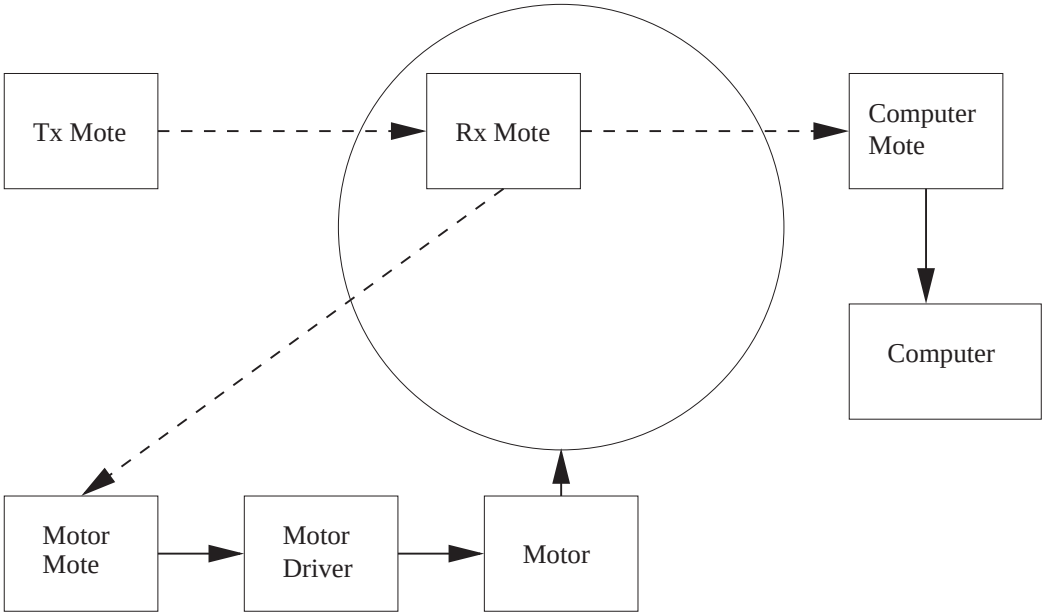

Figure 2.6. The layout of the experiment that tests the search protocols. The dashed lines are the wireless transmissions while the solid lines represent wired transmissions.

2.6 Application of the Search Protocols

I conducted several experiments to test the performance of the search protocols and determine how well they can improve the link quality between two motes. The layout of the experiment is shown in Figure 2.6. Throughout the whole experiment, the Tx Mote would continuously transmit its message at intervals of separated by 60ms. The Rx Mote was placed on the perimeter of the rotating platform and could command the rotation of the platform by communicating with the Motor Mote. Whenever the Rx Mote received a signal from the Tx Mote, it would send the interpreted RSS to the Computer Mote that directly sent the results to the computer that recorded them.

The Rx Mote started with the Global Search protocol by having the platform

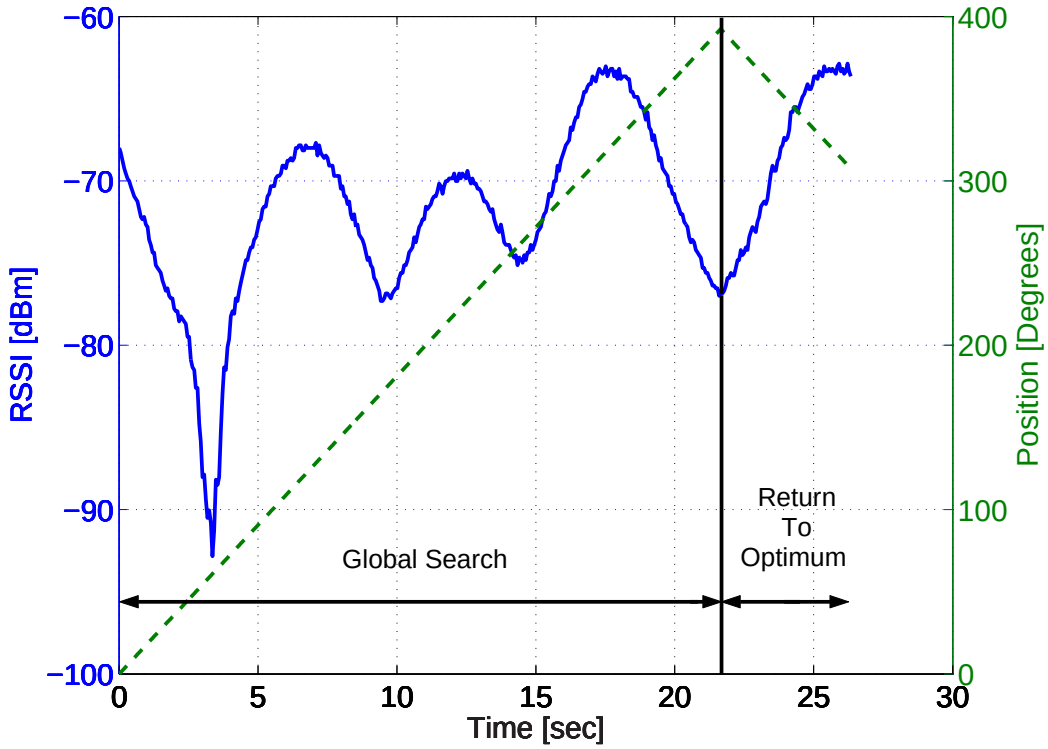

Figure 2.7. The results of the Global Search with the Mica2. The solid line is the sampled RSS and is detailed by the y-axis to the left. The dashed line is the angular position of where the sample was taken and is detailed by the y-axis to the right.

turn continuously, and the mote would take enough samples for a full revolution. In this case, the rotation speed was 21.8sec/rev so approximately 380 samples were needed since the Tx Mote was sending a packet once every 60ms. The mote was placed 28cm from the origin of the turntable so there was a distance of 0.48cm between samples. The results of the Global Search can be seen in Figure 2.7.

For the first 22 seconds in Figure 2.7, the receiver mote does a little more than a full rotation while taking samples. The receiver mote then determines that the best position was the sample that it took at 17.5 seconds and uses the next 4 seconds returning back to that position by making the turntable rotate in the

opposite direction. This is why the regions 17.5 to 22 seconds is a mirror of the 22 to 26 second region.

After the Global Search was complete, the Local Search protocol was engaged. The results of the Local Search can be seen in Figure 2.8. Here, the receiver mote spends the first 4 seconds measuring the RSS of 30 samples of the transmitted signal while having the turntable remain static. It then moved clockwise by $\lambda/16$ and took 30 more samples. It then determined that the new position was worse than the original. The receiver mote then rotated counterclockwise by $2\lambda/16$ and took 30 more samples. It determined that the third position was better than the first so it continued to go counterclockwise by $\lambda/16$. However, this fourth set of samples from 12 to 15 seconds was worse than the third position so the receiver returned back to the third position by rotating clockwise by $\lambda/16$.

This experiment was done with Mica2s that have a carrier frequency of 433MHz with a wavelength of 69cm. This experiment was also conducted with MicaZs to show that limited mobility scales across frequencies. An important consideration is the coherence length which is the minimum possible distance between two samples such that the RSS changes appreciably [39]. In many scenarios, the coherence distance is proportional to the wavelength. Therefore, higher carrier frequencies lead to smaller coherence distance so the spatial distance from peak to valley decreases. Therefore, if the MicaZ receiver mote with a 2.4GHz carrier frequency were to travel the exact same distance as the Mica2 receiver mote, there would be approximately 5.5 times more peaks and valleys seen in the Global Search. The higher spatial diversity arises from the increased number of channel realizations resulting from the higher carrier frequency. This proves useful in that there are more possible peaks, but it is also more sensitive to small changes in distance.

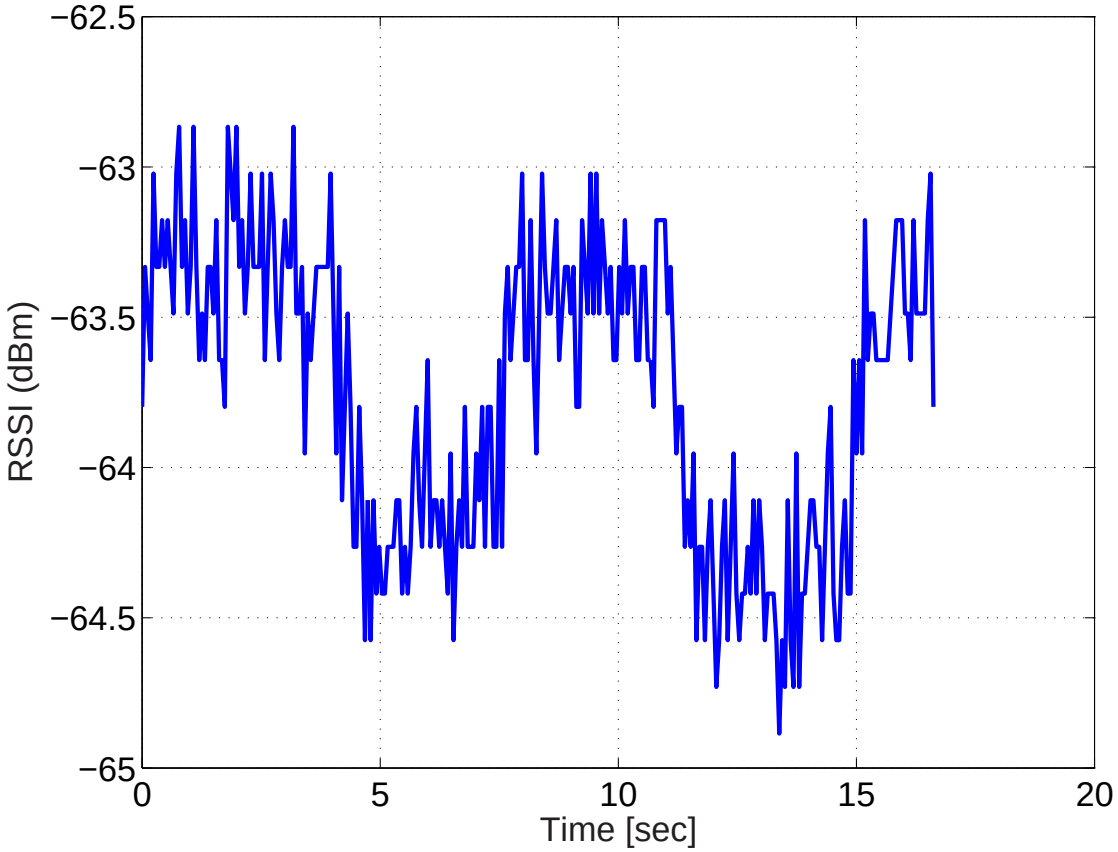

Figure 2.8. The results of the Local Search with the Mica2.

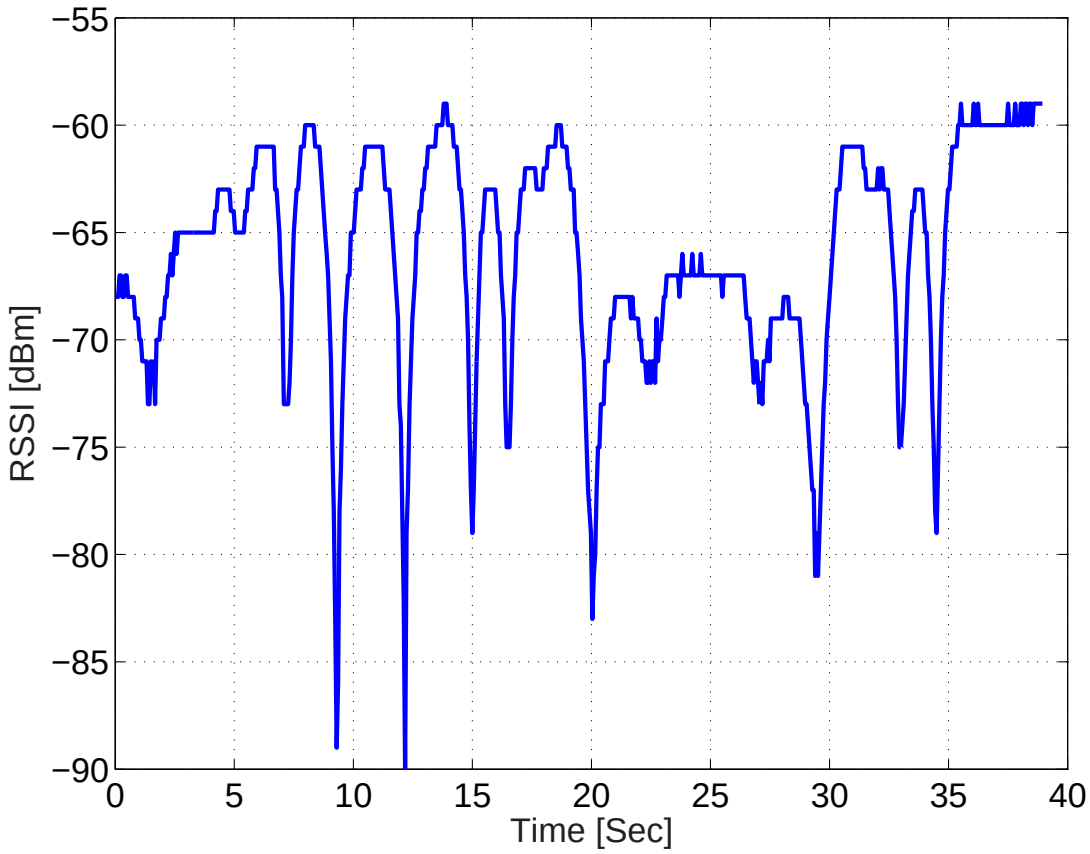

Figure 2.9. The results of the Global Search with the MicaZ. Here, there are more peaks present than the experiment with Mica2.

Higher frequencies require more precision. These effects can be seen in Figure 2.9 where a Global Search was done in a system with MicaZs. The other change was that the MicaZ was placed 12.7cm from the center; therefore, with the increases frequency but shorter distance traveled in consideration, there should be 5.5 more peaks and valleys than in the Mica2 case.

Here, the first 23 seconds are spent in the search stage of the Global Search. The platform remained stationary for 3 seconds and then the platform rotated in the opposite direction for 9 seconds to return to the position with the highest RSS

which was found at the 14 second mark.

2.7 Effectiveness and Results

The environmental condition plays a large role in the overall effectiveness of the mobile receiver. The spatial search protocol always proves to be equivalent or more effective than a MIMO system applying selection combining, but its magnitude of diversity gain depends greatly on the amount of fading present. The Amount of Fading (AoF) described in [18] is a good indicator of how well the mobile receiver will outperform the MIMO system in an given environment.

$$\text{AoF} = \frac{\sigma^2}{\overline{\mathbf{s}}^2}, \tag{2.12}$$

where the numerator is the variance of the power of the channel, and the denominator is the square of the mean of the power of the sampled channel. Therefore, the AoF of a channel demonstrating Rayleigh fading will be 1. When the sampled power of the channel is squared, the Rayleigh distribution becomes an exponential distribution. Here, the variance of the exponential distribution divided by the mean will yield 1 as a result. A large AoF implies that there is large variance relative to the mean. This makes it more probable that the maximum point is located at the apex of a more narrow peak, which, in turn, makes it more unlikely that a MIMO system would sample the position with the strongest link quality while the mobile antenna will find it if it takes enough samples of the overall spatial region. Therefore, a higher AoF implies that the COLMO system will outperform the MIMO system more strongly.

The results of several experiments can be seen in Table 2.1. Experiments 1, 2, and 3 were conducted with Mica2s while MicaZs were used for experiment 4

TABLE 2.1

MOBILE NODE AND MIMO PERFORMANCE

Experiment	1	2	3	4
Maximum RSS (dBm)	-63.2	-72.0	-74.3	-59.0
Average RSS (dBm)	-72.2	-78.1	-78.6	-66.1
MIMO RSS (dBm)	-67.2	-73.4	-75.4	-61.7
Difference (dB)	4.0	1.4	1.1	2.7
AoF	0.29	0.18	0.10	0.23

with the channel shown in Figure 2.9. The row titled "Maximum RSS" shows the RSS of the maximum point in the spatial channel found with global and search protocols. The next row "Average RSS" is the expected RSS if the receiver mote was placed randomly on the perimeter of the turntable. The third row, "MIMO RSS," gives the expected RSS if 4 antennas applying selection combining were placed on the perimeter of the turntable and were evenly spaced apart to form a square. The row labeled "Difference" shows how much stronger the Maximum RSS was in comparison to the MIMO system. The final row displays the calculated AoF of that fading channel.

2.8 COLMO vs. MIMO

Table 2.1 displays the performance of the COLMO system in comparison to the MIMO system. In every case, the Maximum RSS (COLMO system) was superior to the MIMO RSS (MIMO system) as expected. Also, the Difference

value is shown to be correlated to the AoF. A larger AoF gave a larger difference and appears to be a good indicator of how well the limited mobile receiver will outperform the MIMO system. From the table, the Difference is roughly defined as follows:

$$\text{Difference [dB]} = 10 \cdot \text{AoF}. \tag{2.13}$$

In [18], a large AoF value implies that the value for A in (2.8) is very small which implies the Ricean fading with a weak or nonexistent LOS. On the other hand, a low AoF signifies Ricean fading with a larger LOS amplitude. Therefore, the mobile receiver becomes more effective than the MIMO receivers when the spatial channel favors the Rayleigh distribution.

CHAPTER 3

NETWORK APPLICATIONS OF CONTROLLED LIMITED MOBILITY

3.1 Rayleigh Fading Networks

A popular early model for the analysis of multihop networks is the disk model. This model states that two nodes can make a perfect connection if they are within a certain specified distance and no connection is possible if the distance between the nodes exceeds this value. This is a threshold-based model without fading that ignores that the SINR is a random variable [12].

A more accurate concept is present in [48]. Here, there are regions where reception is almost guaranteed to succeed or fail depending on distance; however, there also exists a distance region with a varying probability of reception as a function distance and fading. The transition region model accounts for the variability in packet reception such that the same distance between the transmitter and receiver can have different values for the probability of packet reception. In this case, the distance alone is not enough information to determine the probability of reception and more tests are needed to find the actual value for the probability. This model accounts for the presence of fading in the reception probability. Note that interference does not have to be present for the transition region to exist.

3.2 Mobile Basestation Model

Since fading can greatly affect the performance of a wireless network, the limited mobility scheme introduced in Chapter 2 to find positions with favorable fading can be used to improve network performance. By positioning key nodes throughout the network, better connectivity in vital locations can surmount a multitude of issues such critical nodes, isolated nodes, and weak links.

Since mobility consumes energy which is very limited in most WSNs, the most practical decision would be to give limited mobility to only the BS or certain relay nodes that serve as the backbone of the network. In certain WSNs, it may be possible to give extra energy to the BS and relay nodes that sensor nodes on the edge of the network do not require.

Most papers that have discussed mobile nodes [34] have proposed the application of data mules which are nodes that travel long distances to collect data. Here, the relay nodes have a large amount of mobility and are able to travel close enough to the designated nodes to ensure connectivity. The relay nodes then travel back with this information to the BS. These relay nodes are fundamentally message ferries that physically transport data.

This may be an effective solution for some examples of WSNs that are too sparsely populated, and the nodes are separated by such large distances that direct transmissions are impossible. Also, the form of transportation such as buses on a college campus may allow the relay mote to avoid expending its own energy in the transportation. However, there are several disadvantages to this system that could severely limit the capabilities of the WSN. Latency can easily become a severe issue depending on the time it takes for the relay node to traverse its route. This value can easily vary from several minutes to hours or days. If the

sensor node is measuring vital conditions, the large latency may make the WSN nearly useless. Also, once the relay node is no longer able to continuously move from node to node due to either to energy drain or some other form of failure, the whole WSN may collapse since since all the sensor nodes will become hidden from the BS. Finally, the data mules may be ineffective in rugged terrain where traveling from position to position may prove extremely difficult if not impossible.

The COLMO system detailed in Chapter 2 can enhance the effectiveness of a WSN even though it does not have the abilities of data mules [34] or message ferries [45], [46]. Data mules are able to overcome large-scale shadowing by going physically around the obstacle creating the shadow. Many proposed models that utilize mobility expect the mobile sink to be able to travel far ranges such as in [41], [42], [38], and [40]. The COLMO system does not have that ability, but it can exploit the small-scale fading issues that can be more crippling than shadowing so it can still be practical in sparse and dense networks alike.

The COLMO node may be able to improve its link connections to the nodes that it has one-hop connections with. It also may be possible to use the limited controlled mobility to establish direct connections with motes that used to be several hops away. Some motes may be relatively close to the BS but are unable to directly contact it due to the severe attenuation caused by fading. In this case, the BS may be able to establish an one-hop connection by moving several wavelengths into a favorable fading position. An example is given in Figure 3.1. In the top figure, the two nodes are isolated and must use a relay node for communication. However, if the Rx node is able to vary its position slightly, a direct connection between the two nodes is now possible as demonstrated in the lower part of Figure 3.1. The benefits for this is two-fold. The first advantage is the

newly established one-hop connection which means that the previously used relays no longer have to expend energy transferring packets from the node originally hidden from the BS. The second advantage is that this node can now function as a critical relay node and relieve some of the energy demands from the other critical relay nodes. Therefore, the efficiency of the network increases and, in turn, its overall effective lifespan. While several ideas such as [7] have been proposed to extend the lifetime of the network, *limited mobility* is a novel technique. Finally, the controlled limited mobile BS may be able to increase the network efficiency by finding nodes that were originally fully isolated due to the fading topography of the network.

3.3 Link Connectivity Experiment in 10-Node Network

The following experiment demonstrates the effectiveness of the COLMO BS in a WSN. The motes were placed throughout the room as shown in Figure 3.2, and the BS was placed in the lower left corner. The BS was placed on the edge of the turntable and tested the packet reception probability with the other 10 motes. Once it determines the link quality of each mote, it commanded the turntable to move 11.25°. Each rotation resulted in the BS being moved 14cm or approximately $\lambda/5$ since Mica2s were used in this experiment. This process was repeated until a full revolution was completed.

Figure 3.3 shows the overall reception probability between the BS and all the nodes throughout the room. Missed packets were most often not evenly distributed across the 10 motes. Usually, the drop in reception probability was caused by either one or several motes being a position of deep fade. For example, the reception probability at angle 340° could easily be caused by one node being unable

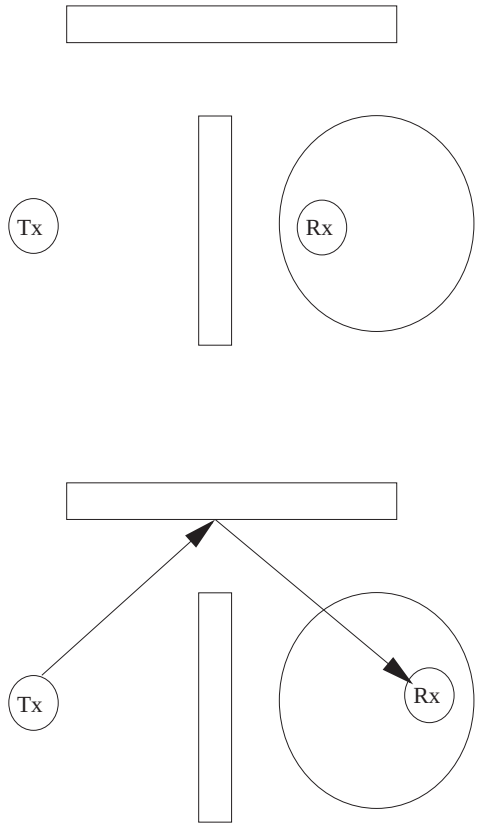

Figure 3.1. Illustration of network connectivity. The top figure shows a case where the Tx node is hidden. The bottom figure shows that a small amount of movement will connect the two nodes.

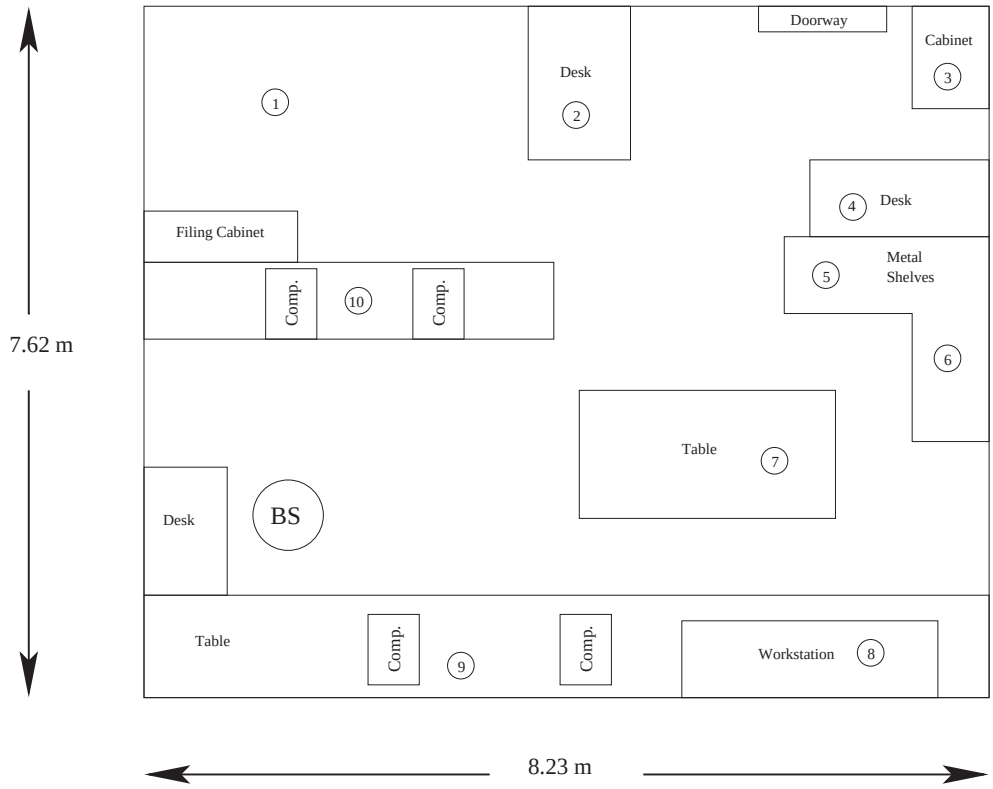

Figure 3.2. The location of the BS and motes throughout the room.

to contact the BS all the time or by 2 motes being able to contact the BS 50% of the time. For Figure 3.3, the ideal location is 30.75° from the original position since this location has the largest reception probability.

Given the probability of reception for each mote at each angle, the most effective metric is:

$$\theta_{Final} = \arg\max_{\theta} \left(\sum_{i=1}^{N} C_i P_i(\theta) \right). \tag{3.1}$$

(3.1) details the ideal location for the BS if only the total packet reception probability is considered. $P_i(\theta)$ is the packet reception probability of mote i when the BS is positioned at angle θ. C_i is the weight or importance given to mote i. This allows the motes to have differing levels of importance depending on outside variables such as how much energy a relay mote contains. For example, a mote may have a large $P_i(\theta)$, but it may not have much energy left so the BS can preserve the lifetime of that relay mote by giving it a low weight. This allows for a level of flexibility that is absent from immobile wireless networks.

When the BS is trying to find a single node that is invisible, it will adjust the weights C_i such that $C_i = \delta_{ij}$ where mote j is the mote of interest for the BS. Here, (3.1) simplifies into:

$$\theta_{Final,j} = \arg\max_{\theta} \left(P_j(\theta) \right) \tag{3.2}$$

θ_{Final} can vary depending on which mote that the BS is seeking. For example, Figure 3.4 displays the packet reception probability for mote 9. Here, almost all possible positions for the BS have favorable multipath fading except for one small region surrounding 80°. In this small region of deep fading, the mote 9 is completely hidden from the BS. For this case, only a small amount of movement

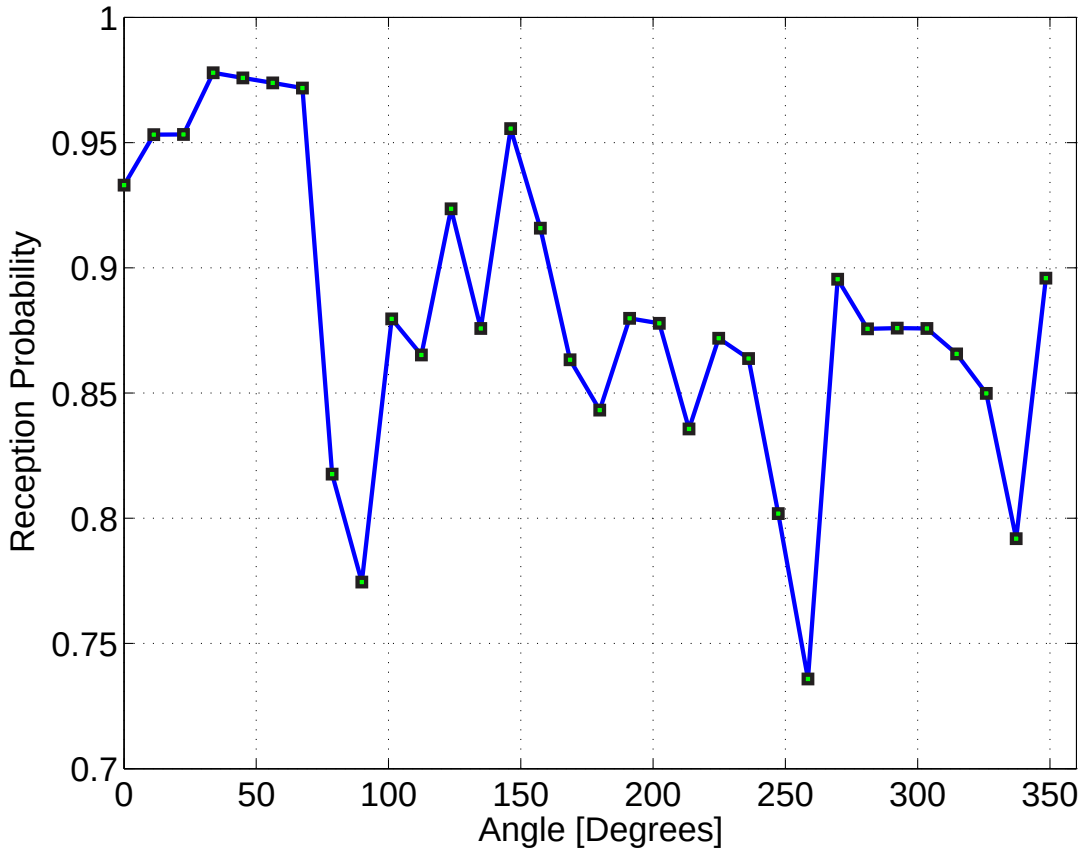

Figure 3.3. Reception probability for all the motes as a function of the position of the BS.

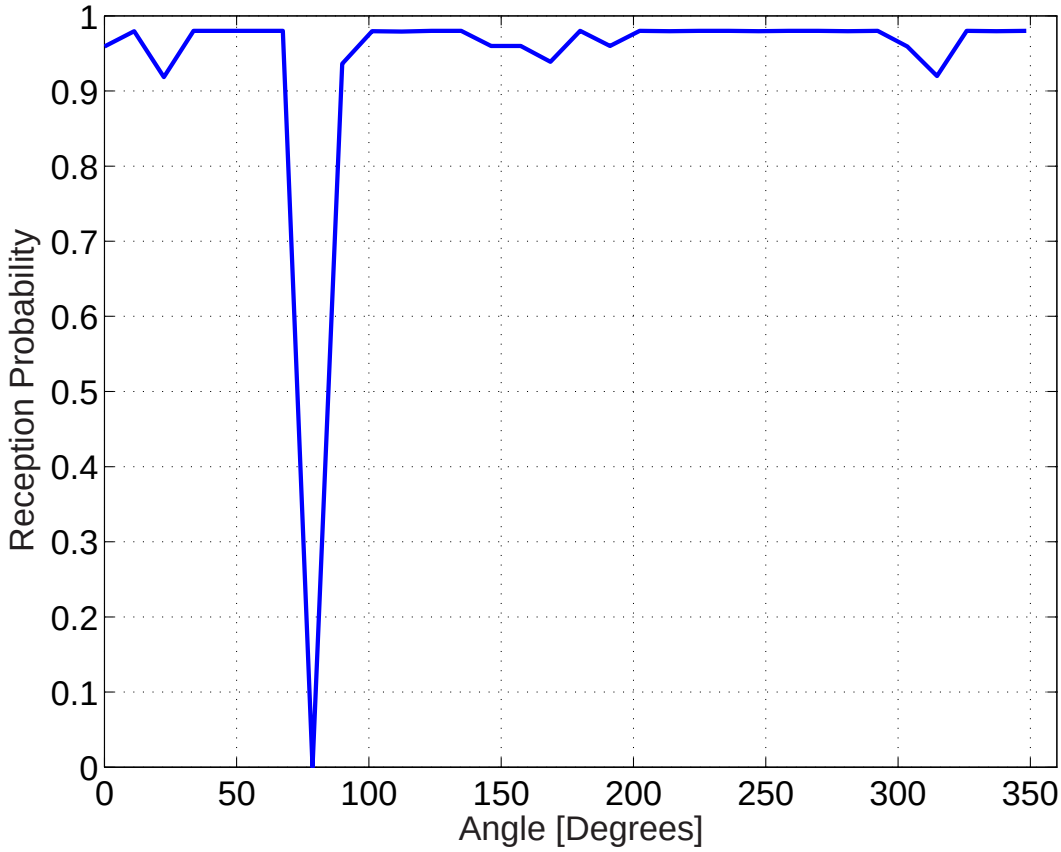

Figure 3.4. The reception probability between mote 9 and the BS.

is needed for the BS to have dramatically better link quality.

Mote 3 shows another situation where high reception probability is much more difficult to find. In Figure 3.5, it is far more likely for the BS to be in a position where it has a poor link quality to mote 3. If the BS was placed randomly anywhere on the each of the turntable, mote 3 would with good probability either be invisible or have a poor connection. However, if the BS has limited controlled mobility, it can find a position with very good link quality. With this ability, the BS can turn a mote that was possibly separated by several hops into a potential critical node in the network. This allows the distribution of the energy draining

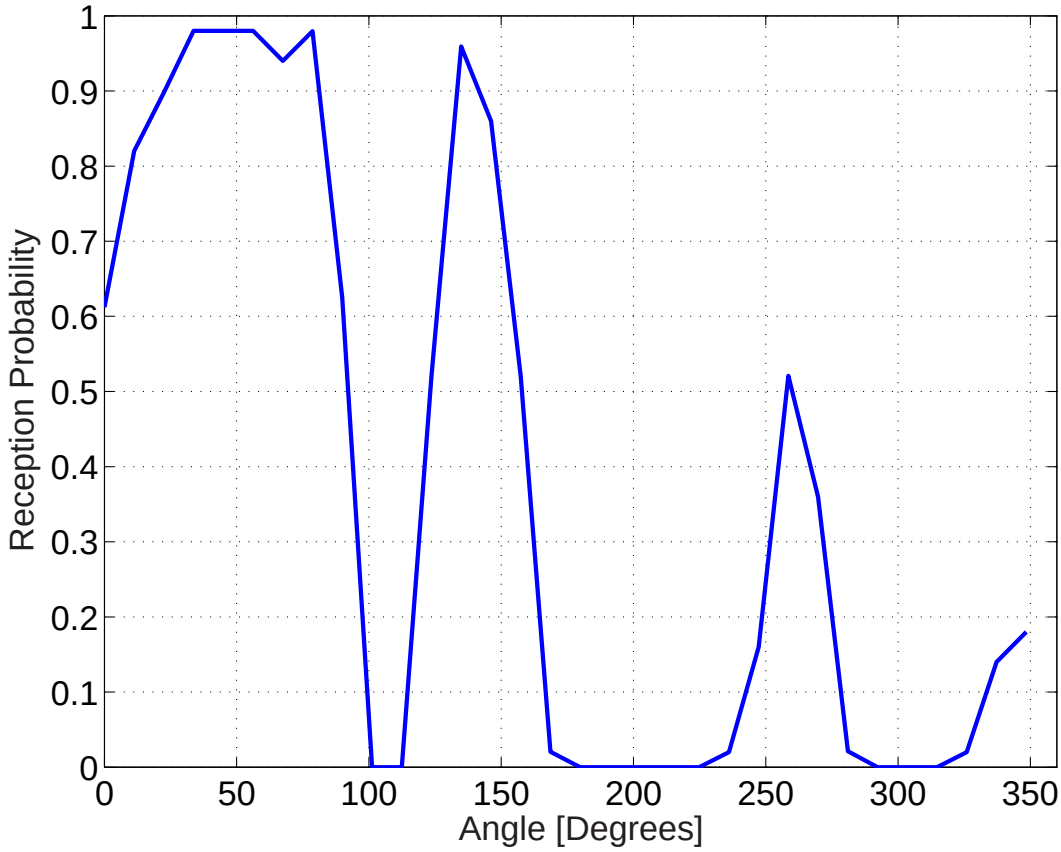

Figure 3.5. The reception probability between mote 3 and the BS.

responsibilities of the critical nodes across a larger set of nodes and thus, extend the lifetime of the network.

Since the spatial fading patterns of the motes with the BS are mostly uncorrelated with each other, the BS may have limited positions where it has a strong link quality with several motes simultaneously. Each of the motes will have its own unique spatial fading patterns with varying locations for the favorable fading and destructive fading. For example, motes 3, 5, and 9 have different spatial fading patterns that are uncorrelated since they were placed several meters apart which is several times the wavelength of the carrier frequency of the Mica2. If only motes

3 and 5 were to be considered, then the range 31° to 75° would have been useful. However, if we are to consider motes 3, 5, and 9 simultaneously, then the range will be decreased to 31° to 65°. This implies that there is an upper limit to how many motes can have one-hop connections to the BS even with controlled limited mobility.

Although it is unlikely for the mobile BS to find a position where it can reach all the nodes, its limited mobility does allow the network to be more robust and efficient. Different positions will allows the BS to communicate with different sets of nodes since some positions will reveal certain nodes while isolating others.

The expected number of motes one-hop away from the BS is explored in [13]. In this work, the nodes are distributed via the Poisson point process of intensity 1. It explores the connectivity of a uniformly distributed network of infinite size with Rayleigh fading between all the motes. When the path loss exponent is equal to 2, the expected number of motes one hop away from the BS is given by:

$$\mathbb{E}[n] = \sum_{k=1}^{\infty} \mathbb{P}[C_k] = \frac{\pi}{s}, \tag{3.3}$$

where C_k is the event that mote k is connected to the BS, and s is the path gain threshold which can also be considered as the SNR threshold needed for a connection between the two motes to be established. The equation for the expected number of motes connected to the BS becomes more complex when the path loss exponent is not equal to 2 [14]. The expected value of nodes is independent of the position of the BS in the network. However, this is only true for infinite networks. For finite networks, as our experiments show, the connectivity of the BS depends on its position.

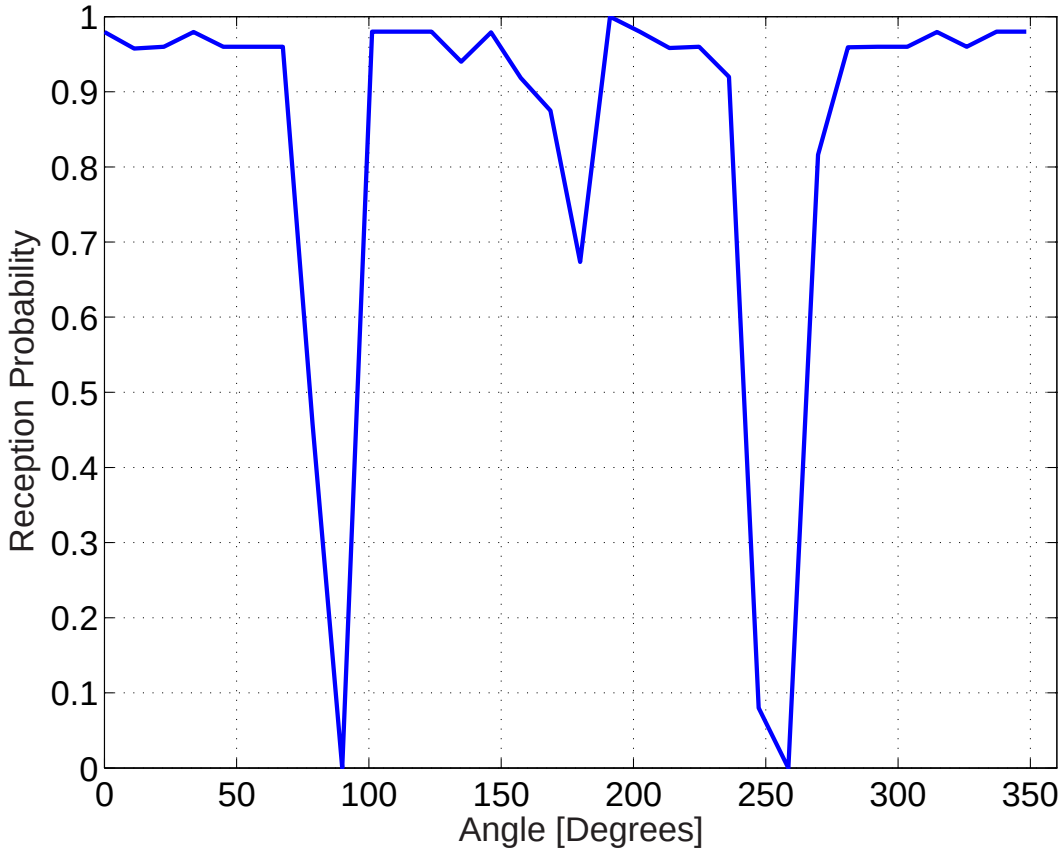

Figure 3.6. The reception probability between mote 5 and the BS.

3.4 Relay Experiment

Relay nodes may also enhance the overall network efficiency with the application of controlled limited mobility. While it may not be practical to give limited mobility to all the relay nodes in a network, it may prove useful for some relay nodes in the backbone of the network especially in the bottleneck regions. The use of COLMO relays and a COLMO BS allows the mobility to scale with the size of the network. It is unlikely the BS will be able to communicate with every relay and sensor node especially if the network consists of thousands of such nodes. However, the application of several properly located mobile relays can allow the benefits of the limited mobility to penetrate the whole network. First, the COLMO relays on the edges of the network would adjust themselves properly for the most effective performance in the network, and the COLMO relays one-hop closer to the COLMO BS would adjust themselves afterwards. This would continue until the COLMO BS finally adjusts itself accordingly.

The following experiment shows the effectiveness of a COLMO relay node. Here, the goal was to get two motes, Mica2s labeled Tx1 and Tx2, to share a strong RSS by applying a relay, Rx1. The RSSI was used to test the link quality between since it requires fewer samples to test the link quality in comparison to directly testing for the packet reception probability. This allows the relay to quickly test the link quality and find the best position. Using the RSSI also shows that the Global Search protocol demonstrated in Chapter 2 can be used for relays and the BS.

The overall experiment took several stages. In the first stage, the relay node was ignored, and Tx1 sent a packet directly to Tx2 once every 200ms as pictured in Figure 3.7. Tx2 then interpreted the RSS of the received packet and then wait

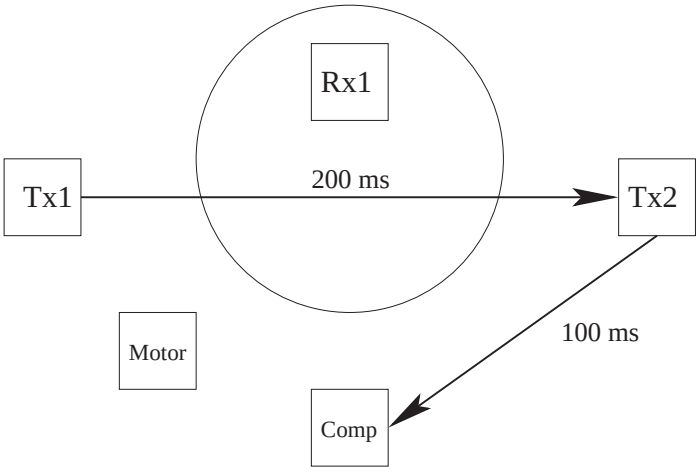

Figure 3.7. Stage 1 of the relay experiment. The relay node is ignored by Tx1 and Tx2.

100ms before it sent its interpreted data to the mote attached to the computer. This delay ensured that there was approximately 100ms between each packet being delivered. It is possible for packets to be dropped due to collisions if the delivery rate was more than 20packets/sec, so a 100ms interval time appears to be a safe value. For this experiment, the average RSS for the link between Tx1 and Tx2 was -67.7dBm.

After stage 1 was completed, the system engaged stage 2 which is displayed in Figure 3.8. The purpose of this stage is to determine the fading channel between Rx1 with Tx1 and Tx2 in relationship to Rx1's position. At the beginning of Stage 2, Tx1 informs the motor to continuously rotate the turntable containing Rx1. After this, Tx1 then continuously sends a packet every 300ms. This packet has two different destinations. The first destination is Rx1 which then interprets the RSS between it and Tx1. The second destination of Tx1's packet is Tx2. Once Tx2 receives the packet, it waits 100ms and then sends its own packet to

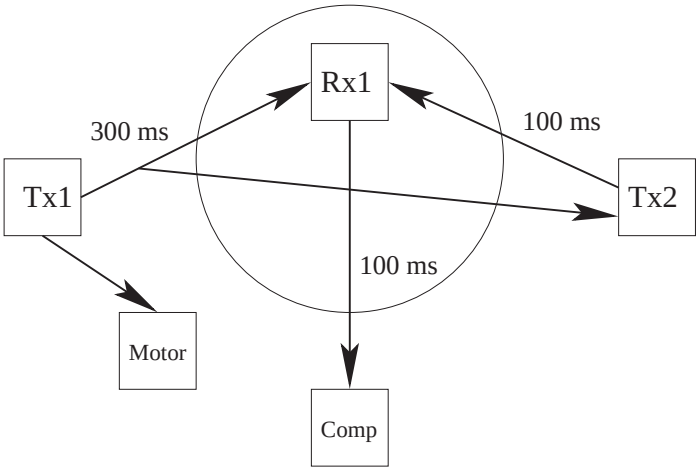

Figure 3.8. Stage 2 of the relay experiment. Rx1 conducts a Global Search for both Tx1 and Tx2.

Rx1. Therefore, Rx1 is able to get the RSS from Tx1 and Tx2. It then stores these values and sends them to the mote connected to the computer 100ms after receiving the value from Tx2. This setup once again assures that each of the packets sent are separated by 100ms to avoid collisions. This is done for a full rotation of the turntable so that the full scale of the fading channel can be seen.

The results of the fading in relationship to the position of the relay node can be seen in Figure 3.9 where the solid line is the RSS between Tx1 and Rx1 while the dashed line is the RSS between Tx2 and Rx1. A compromise is needed for the relay node to be an effective alternative. The maximum RSS for the channel between Tx1 and Rx1 is -56.2dBm while the max between Tx2 and Rx1 is -54.2dBm. However, the maximum point is not in the same location for these two channels. In fact, the position with max value for the second channel at 290° yields a very poor value for the first channel. One technique to determine the best position would be to determine:

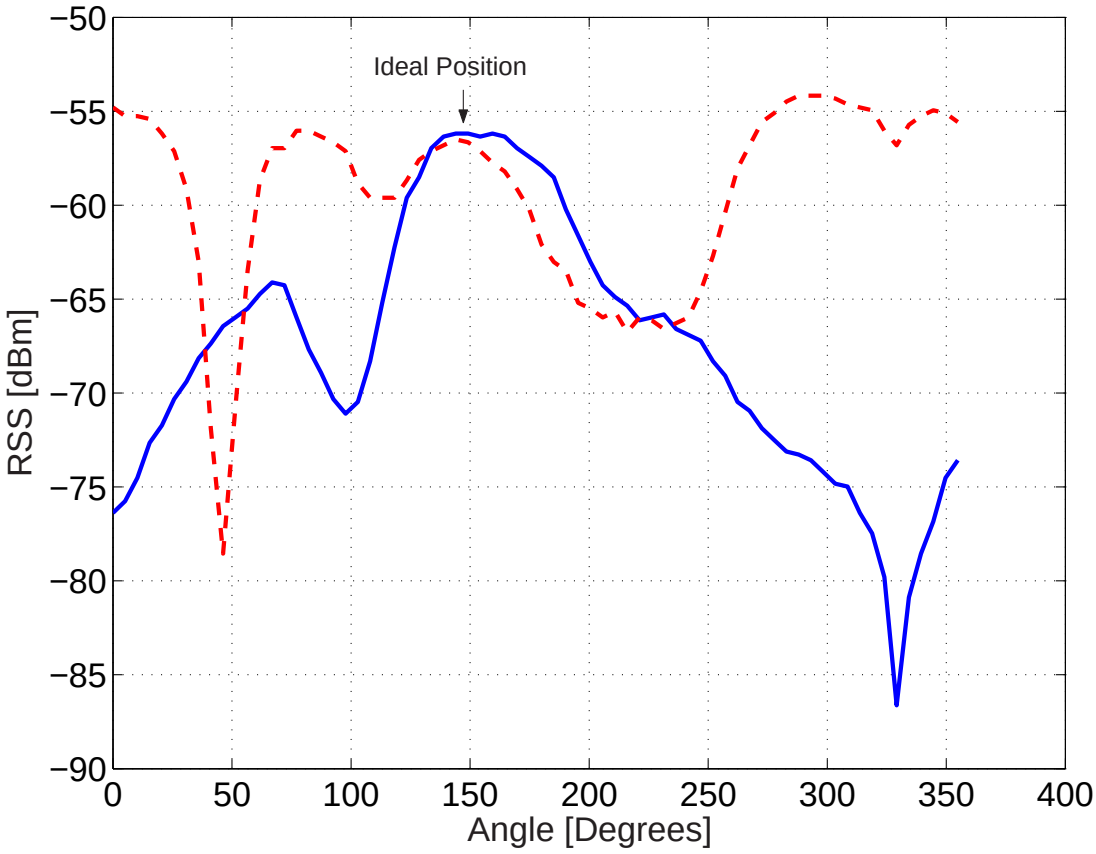

Figure 3.9. Signal strength of both channels. The solid line is the RSS of Tx1, and the dashed line is the RSS of Tx2.

$$\theta_{Final} = \arg\max_{\theta} \left(\min_{i} (S_i(\theta) \right). \tag{3.4}$$

It takes the minimum RSS sample from each position and then finds the position with the largest minimum RSS. The minimum RSS of the channels for each position can be seen in Figure 3.10. This technique is effective at avoiding deep fades for both Tx1 and Tx2. Here, the ideal position is 145° since it has the largest minimum RSS of both channels. At this position, the RSS for the first channel is -56.2 dBm, and it's -56.5dBm for the second channel. If the relay node did not have controlled limited mobility, the expected RSS for the first channel would be -67.7dBm which is not much better than the original -69.7dBm. Ironically, the relay node would have been detrimental since it would have added an extra hop in the route.

Once the ideal position for Rx1 is determined, the system enters Stage 3 where Rx1 tells the motor to rotate back to the position where Rx1 found the best RSS average for the two channels. Once Rx1 returns to the ideal location, it remains stationary and sends out a command to Tx1 and Tx2 to go into the final stage. In stage 4, Rx1 acts as a relay for Tx1 and Tx2 as shown in Figure 3.12. In Figure 3.12, Tx1 sends a packet to Rx1 once every 100ms. Once Rx1 gets the packet from Tx1, it waits 100ms and sends the packet to Tx2. Tx2 also waits 100ms and sends the data to the Mica2 mote connected to the computer. The extended wait times, 100ms, between each packet was maintained to ensure that the packet drops were not caused by collisions.

Since the COLMO receiver has shown to be able to work as a BS or relay node and can scale for larger WSNs, it can be used to improve many routing protocols. For example, the routing protocol that determines routes with the least

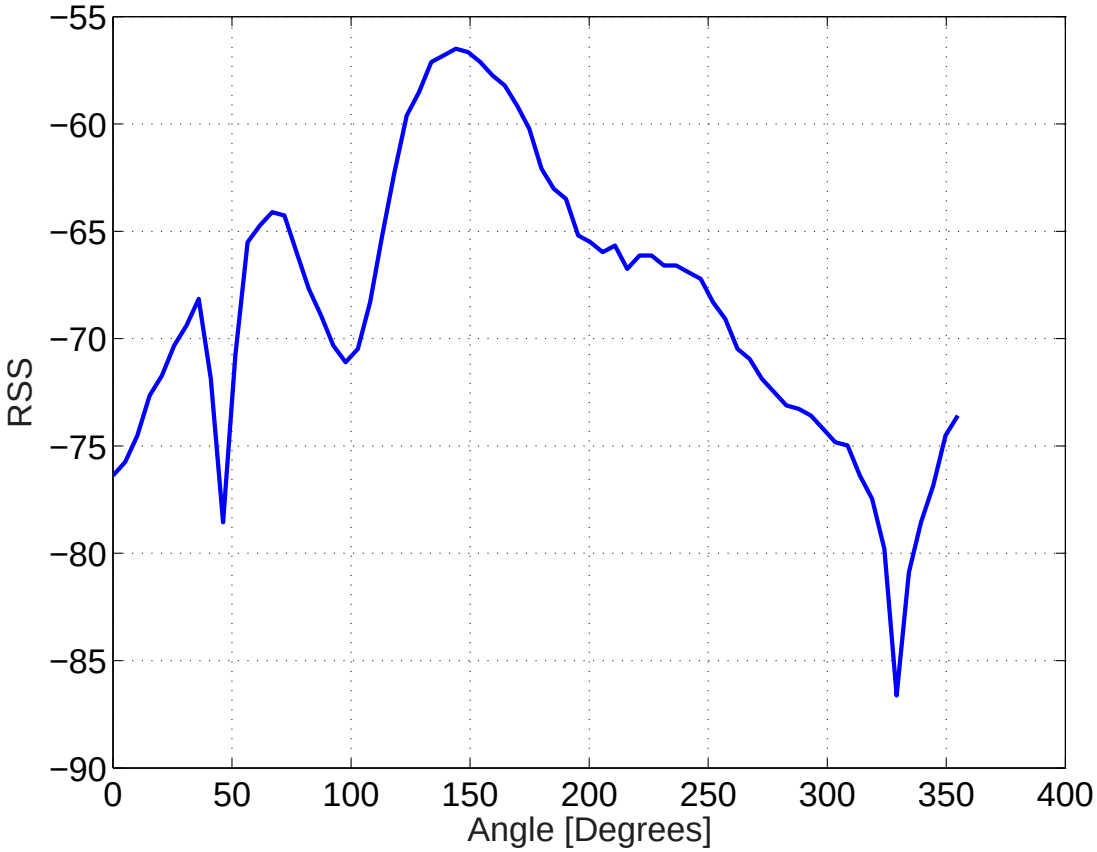

Figure 3.10. Minimum signal strength from each position in Figure 3.9

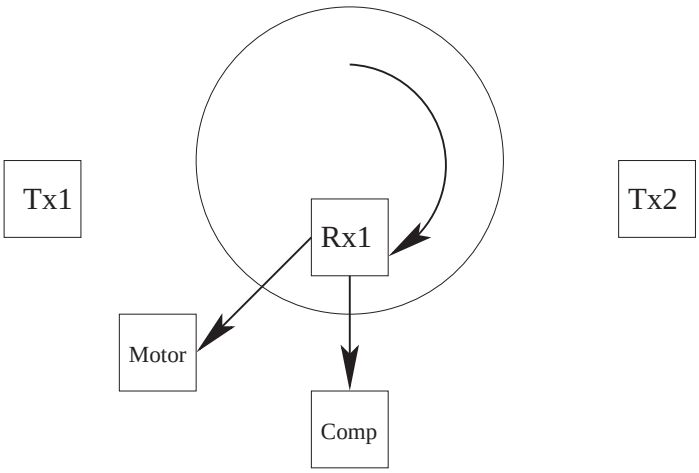

Figure 3.11. Stage 3 of the relay experiment. Rx1 is returning to the position with the highest average RSS.

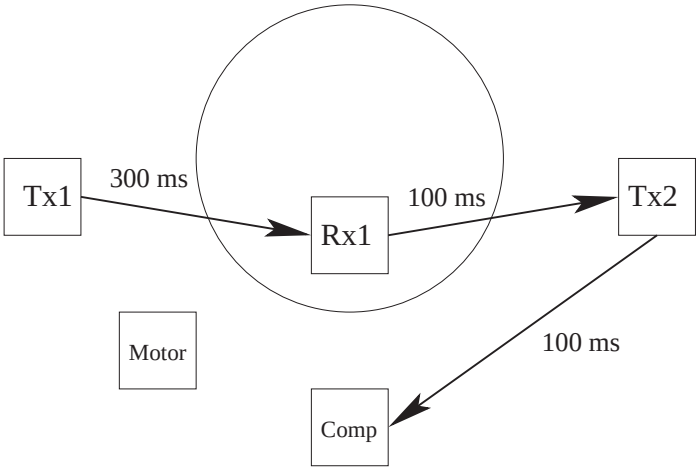

Figure 3.12. Stage 4 of the relay experiment. Rx1 is serving as a relay between Tx1 and Tx2.

required numbered of transmissions, or the ETX metric described in Chapter 1, could be modified to apply controlled limited mobility. The ETX metric may ignore certain routing paths since certain links in the proposed metric may have very poor reception probability. These links may be improved with the mobile nodes so the ETX metric may have new paths to consider that were originally impractical.

The min-hop metric could also find the mobile nodes system to be greatly beneficial. Many research efforts such as [6] have shown that the min-hop metric is a very poor metric since it does not consider the probability that the packet will be successfully transmitted across the network. However, the improvement in link quality through limited mobile nodes may make the min-hop metric a viable option for some networks.

CHAPTER 4

PERFORMANCE METRICS FOR LINK QUALITY ESTIMATION

4.1 Link Metrics

Since mobile nodes consume energy every time they move, it is ideal to keep the total required number of movements to a minimum. Therefore, the node needs to find the ideal position where it will best serve the network for the longest time possible before it needs to move again. When the mobile node is testing the link quality for a certain position, it needs to rely on a link quality metric that accurately tells the link quality of the position and how robust the link will remain in that area if there are changes in the surrounding environment [20]. Also, the total sampling time required to determine the link quality will be an important characteristic of the chosen metric. If it takes too long to thoroughly sample the link quality, the mobile system may prove impractical if the fading environment is time-variant to even an small degree.

4.1.1 Packet Reception Rate

One of the more basic techniques to determining the link quality of a certain position is by simply determining outright how often a packet will be dropped, *i.e.*, empirically evaluating the packet reception rate. The mobile node counts

how many packets are dropped versus the number of packets that were sent and determines the link quality accordingly.

An advantage to this metric is that it gives an insight to the frequency and variations for dropped packets. In some links, the probability that a packet will be dropped is independent of the success rate of the packets that are sent before and after said packet. However, there are situations where the errors are more likely to occur in bursts. These groups of errors usually prove to be more detrimental in networks versus the cases where the errors are independent and uniformly distributed. One such metric was proposed in [5]. Here, bursts of errors penalize the channel by lowering the value of the link quality.

Conversely, the disadvantage of applying this metric is the long sample time required. Many samples would be required to accurately portray the channel link quality. This issue is compounded since this test has to be repeated over several different locations before the mobile node can determine the ideal location. This extra amount of time can lead to longer latency in the network and long periods when the relay node is not transmitting packets since it is too busy analyzing the link quality of its position.

4.1.2 Link Quality Indicator

A relatively new metric is the Link Quality Indicator (LQI). This can be used by appliances adhering to the Zigbee standard such as the MicaZs. The LQI operates by taking the sample error rate of the first 8 chips of a packet and then calculates likely package drop probability.

The LQI is very good indicator of the quality of the link since it can determine very closely the actual package reception rate (PRR). However, it still needs to

average many samples of the LQI to determine the PRR so latency can still be an issue. Also, the LQI is not available for all systems such as the older Mica motes so it may not even be an option for some WSNs. Also, it cannot determine the distribution of the packets being dropped. Channels that drop packets uniformly throughout time or those that drop them in groups are equally penalized as long as they drop the same average number of packets.

4.1.3 Received Signal Strength Indicator

An older procedure is to calculate the signal strength of the packet being received, and positions that receive packets with the largest signal power should be favored. Even older systems such as the Mica2s can determine the RSS of the received packets so this metric can be used for many different types of WSNs. Also, it only requires the average of only a couple of samples so it results in smaller latency than the previous two metrics. In fact, it is stated in [37] that often enough variance is so small that sometimes even a single packet will be sufficient. This rapid analysis of the link quality would be vital for WSNs that use COLMO nodes and need low latency. Since the spatial variations of the channel can be analyzed so quickly, it may also be possible to be searching for a better position at constant intervals. This would allow to the mobile node to be adaptive even in environments where the fading channel is periodically changing, an important ability that is emphasized in [43].

However, the RSSI is not always precise in determining the actual PRR. The correlation between the RSS and the PRR is weaker than between the LQI and PRR. In fact, many have considered it to be a poor indicator as shown in [37]. Only a small range of the RSSI scale, several dBm above the noise floor, can

be used to determine the strength of the link quality. RSS values higher than this range usually imply perfect PRR while RSS values below the noise floor will be missed since the packet will be dropped. Regardless, the RSSI has enough correlation with the PRR to find positions for the mobile node that are favorable, but it still may not have enough correlation to detect the more questionable fading patterns. The RSSI is able to detect the good channels, but it poorly detects the link quality of mediocre or poor channels.

4.2 Experimental Analysis of the Performance Metric

I conducted a trial similar to the BS network experiment in Chapter 3 to test the performance of each metric. I conducted this test with MicaZs since they can simultaneously measure the RSSI and LQI of a received packet. The BS and its rotating platform was placed in the center of the room, but the mote that it was trying to contact was hidden behind several metal plates so fading from multipath was prevalent. The BS transmitted a packet to the mote and then wait for the reply. If the mote was not able to hear the BS or the reply from the mote was dropped, the BS recorded the event as a missed packet. If the BS was successfully able to hear from the mote, it recorded the event as a successful packet reception and measured the RSSI and LQI of the received packet. The BS tested each transmitting mote in the network in order via polling. The BS conducted 100 packet tests from each transmitting mote and then move 18° and repeat the test until a full revolution was conducted. The results can be seen in Figure 4.1.

The plot on top is the resulting PRR, the solid line, with the averaged LQI, the dashed line, superimposed so that the nearly perfect correlation can be easily seen. Note that the LQI value was normalized. The slight differences results from

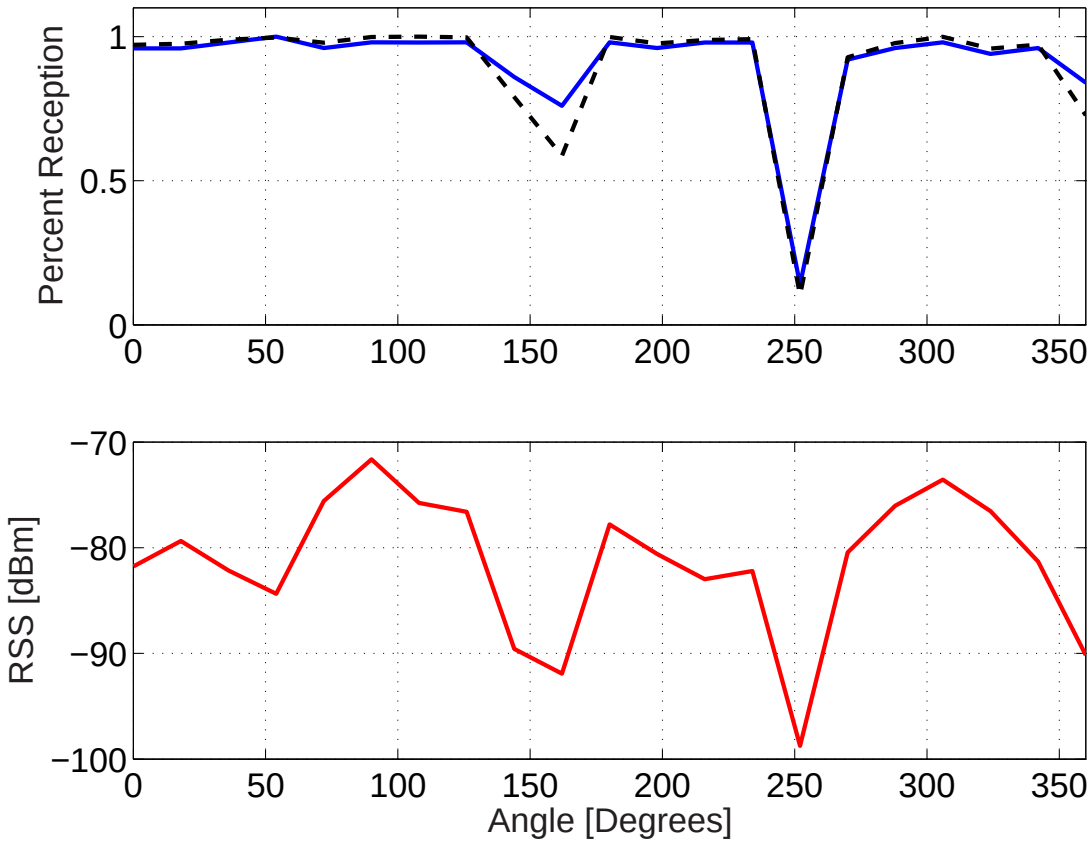

Figure 4.1. The top graph shows both the PRR, solid link, and the LQI, dashed line. The bottom plot displays the RSSI.

the averaging window not being large enough to remove the effects of the variances in the set of measurements. Other than for a couple of positions, the two values overlap throughout nearly the whole test.

The lower plot is the resulting RSSI for the same positions. The correlation between the RSSI and PRR is relatively weak but there is enough allow the RSSI to be a useful indicator. The RSSI was able to predict the large dips in the PRR especially at the positions 160° and 250°. However, the RSSI displays a large variance for positions where the PRR indicates an excellent link quality.

While the RSSI does display a large variance especially for positions with mediocre link quality, it does indicate the positions with poor link quality, and it provides insights to the positions with high link quality. For example, the PRR and LQI samples indicate that almost any position other than those surrounding 160°, 250°, and 355° are favorable. However, the RSSI is able to glean more information about the link quality for each position. The noise sensitive floor for the MicaZ is slightly lower than -90dBm, and any packet received with a weaker signal strength will most likely be dropped. Also, packets close to the noise floor may have a low PRR because any variance in the RSS that lowers the signal strength will cause the packet to be lost. The higher the RSSI, the less likely that a packet sent at that position is dropped. Therefore, the RSSI plot shows that the position at 90° will be the most favorable since it has the highest RSSI value. Even the positions adjacent to 90° also have very favorable PRR, they give no more information about the robustness of that position. Since the potion at 90° has the highest RSSI, it is possible that it is the most robust and protected position against changes in the environment. For example, if some of the objects in the lab were moved around, the resulting RSS could greatly vary. However,

since the position at 90° is the farthest one from the noise floor, it is the one least likely to drop down to the noise floor after the surrounding environment is modified.

There are several factors that need to be considered when measuring for the RSSI and LQI. First, these measurements do not take into account of interference from motes throughout the network. Therefore, the mote may not be able to take into account the SINR of the received signal. Second, the RSSI and LQI measurements were taken only by the packets that the mote was actually able to receive and not the packets that were so weak that they were dropped. Since the dropped packets were not able to be considered, the true RSSI and LQI values are usually lower than the ones that were sampled. For example, the noise floor for the MicaZs is approximately -100dBm; therefore, any received packets with a signal strength less than -100dBm will be dropped and ignored. Although the averaged RSSI could be sampled to be -95dBm, the true averaged may RSSI could be -105dBm or even lower. This can be an important issue to consider when the link quality is exceptionally poor.

CHAPTER 5

SPATIAL SAMPLING RATE AND INTERPOLATION

5.1 Sampling Concerns and Issues

When a mobile BS or node is searching for the best position, it is not serving the rest of the network. Therefore, the more time required for the COLMO node to find the best fading position lowers the overall efficiency of the network. If the mobile node is able to quickly find the position with the best fading, it can attend to its role in the network, and it can more quickly adapt to the changes in the link quality by rapidly finding a new position.

The effective solution is to keep the required number of positions to be sampled between the transmitting nodes and the mobile node to a minimum. Fewer tests of the link quality allows the mobile node to complete a full revolution more quickly. If the spacing between each position is too minute, the fading function (see (2.2)) is oversampled. The node is penalized with more sampled positions than is actually needed since the link quality of the positions surrounding the position being sampled are all strongly correlated [31], [10]. As the distance from the sampled position is increased, the correlation in link quality weakens. Therefore, the next sampled position needs to be far enough away that the correlation between the two positions is weak enough to justify another link quality test. Otherwise, too much energy and time is lost to get nearly the same amount of information of

the spatial diversity of the channel. Conversely, there is the danger of undersampling such that there is too much distance between each position being analyzed. In this case, much of the information in the fading function is lost and cannot be used in the consideration of locating the position with the best link quality. Here, the effectiveness and the diversity gain of the mobile node can be greatly decreased. The compromise is find a sampling rate such that oversampling is kept to a minimum while undersampling is avoided entirely.

The Fourier transform of the sampled channel of the fading coefficient may yield information on the minimum sampling rate. The spatial nature of the fading can be expressed in the frequency domain as shown in [28]. In the frequency domain, the Nyquist sampling rate may show the minimum sampling rate allowed.

5.2 Interpolation Techniques

If the information of the spatial channel is not lost due to undersampling, it is possible to determine if there are favorable points in the regions between the sampled positions via interpolation. Interpolation may be used to find the unsampled signal strength peak through the information found with the adjacent sampled points.

Several different types of interpolation techniques are available with varying levels of effectiveness. One popular technique is the Nyquist Interpolation where the samples are convolved with the sinc function as follows:

$$x(t) = \sum_{n=-\infty}^{\infty} x[n] \cdot \text{sinc}\left(\frac{t - nT}{T}\right) \tag{5.1}$$

Here, $x(t)$ is the reconstructed signal, and $x[n]$ is the value for the sample taken at position n. Here, we are trying to reconstruct a waveform defined over

space instead of time; therefore, the variable T is substituted with $\Delta\theta$, the distance between samples. This is the ideal reconstruction method for stationary waveforms where the distance between samples is small enough to avoid violating the Nyquist criterion. The Nyquist criterion states that the distance between samples must be less than half the inverse of the bandwidth of the waveform [22].

Another useful and possibly applicable interpolation technique is the cubic spline. It has been proven to be an effective curve tracing tool and can accurately recreate the spatial channel if enough samples have been taken. However, there are several factors that may make it prohibitive for certain scenarios. It can be computationally intensive and require more computational ability than what is present in the nodes in most WSNs. Also, this computational demand increases when more samples of the channel are conducted.

Although the cubic spline interpolation is an effective curve tracing technique, we do not need complete knowledge of the spatial channel for an acceptable level of efficiency. We do not need to know exactly the value of the maximum signal strength obtainable. We just need the value of the location of the maximum signal strength so that the mobile node can return to that location. For this, 3-Point Interpolation may prove sufficient in most situations. This technique is computationally inexpensive and can be implemented with relatively simple nodes in the WSN. After the mobile node finishes its Global Search, it determines which of its sampled positions had the highest RSS. Then it determines the positive slope between the point previous to the max point and the max point, and then sums it with the negative slope between the max point and the point afterwards. The result will be divided by the absolute value of the larger slope to normalize the result. Therefore, if the first slope is steeper than the second, the assumed

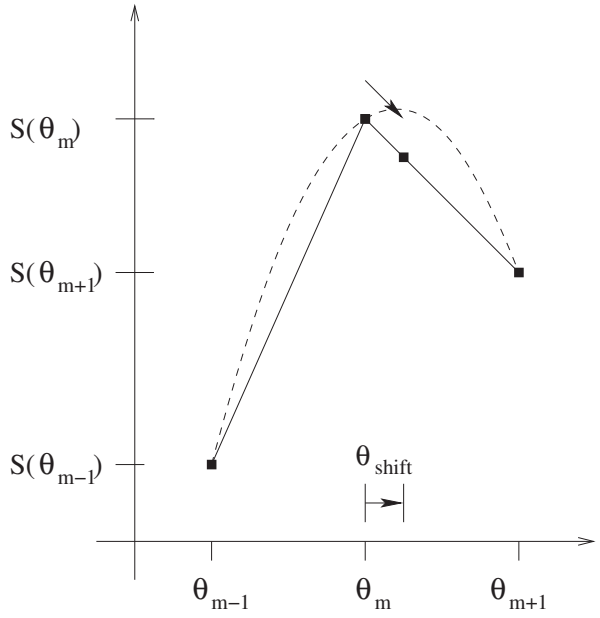

Figure 5.1. Example of the 3-Point Interpolation.

max point will be shifted closer to the point at θ_{m+1}; otherwise, it will be shifted towards θ_{m-1}. The resulting formula is expressed as:

$$\theta_{Shift} = \frac{S(\theta_{m+1}) - S(\theta_{m-1})}{\max[(S(\theta_m) - S(\theta_{m-1})), (S(\theta_{m+1}) - S(\theta_m))]}, \tag{5.2}$$

where $S(\theta_m)$ is the maximum RSS measured. $S(\theta_{m-1})$ is the RSS of the point measured just before the point with max RSS, and $S(\theta_{m+1})$ is the RSS of the point after.

An example of the 3-Point Interpolation is illustrated in Figure 5.1. In this case, the slope obtained by the points θ_{m-1} and θ_m is larger than the slope created by θ_m and θ_{m+1}. This causes the θ_{shift} value to be positive, and the position that is interpreted of having the maximum RSS is at $\theta_m + \theta_{shift}$.

5.3 Analysis of the Sampling Rates and Interpolation

A sampling test was conducted with Mica2s to determine the optimum sampling rate and the performance of each interpolation technique. First, I measured the spatial diversity of the channel by allowing the node on the turntable to make one full revolution while a stationary transmitter was sending a sample every 60ms. The distance between each sampled point was 0.484cm, a very small fraction of the carrier wavelength of 69cm. At this point, the channel is greatly oversampled where each point is highly correlated with the points adjacent to them. The result can be seen in Figure 5.2.

Figure 5.3 shows the resulting fast Fourier transform of the sampled channel after a moving average filter was applied to remove the high frequency noise. The DC component was removed so that rest of the power spectral density could be more easily interpreted. For this test, the minimum sampling rate is approximately 0.425Hz since the values past this point are produced by noise. Due to the dimensions of the turntable used in this experiment, the sampling rate of 0.425Hz translates to a distance of 20.3cm between samples.

I downsampled the channel by 10, 20, 30, 40, and 50 so that the distance between each point was 4.84cm, 9.64cm, 14.4cm, 19.0cm, and 23.5cm respectively. The result of the channel downsampled by 50 is shown in Figure 5.4 where the solid line is the oversampled channel and the dashed line is the downsampled channel. I then measured how far the downsampled position with the max RSS was from the position with the max RSS of the greatly oversampled case.

The Nyquist interpolation results proved to be unsatisfactory. The result of the interpolation for the downsampled by 30 case can be seen in Figure 5.5. The resulting reconstruction is able to reconstruct to the waveform to a moderate

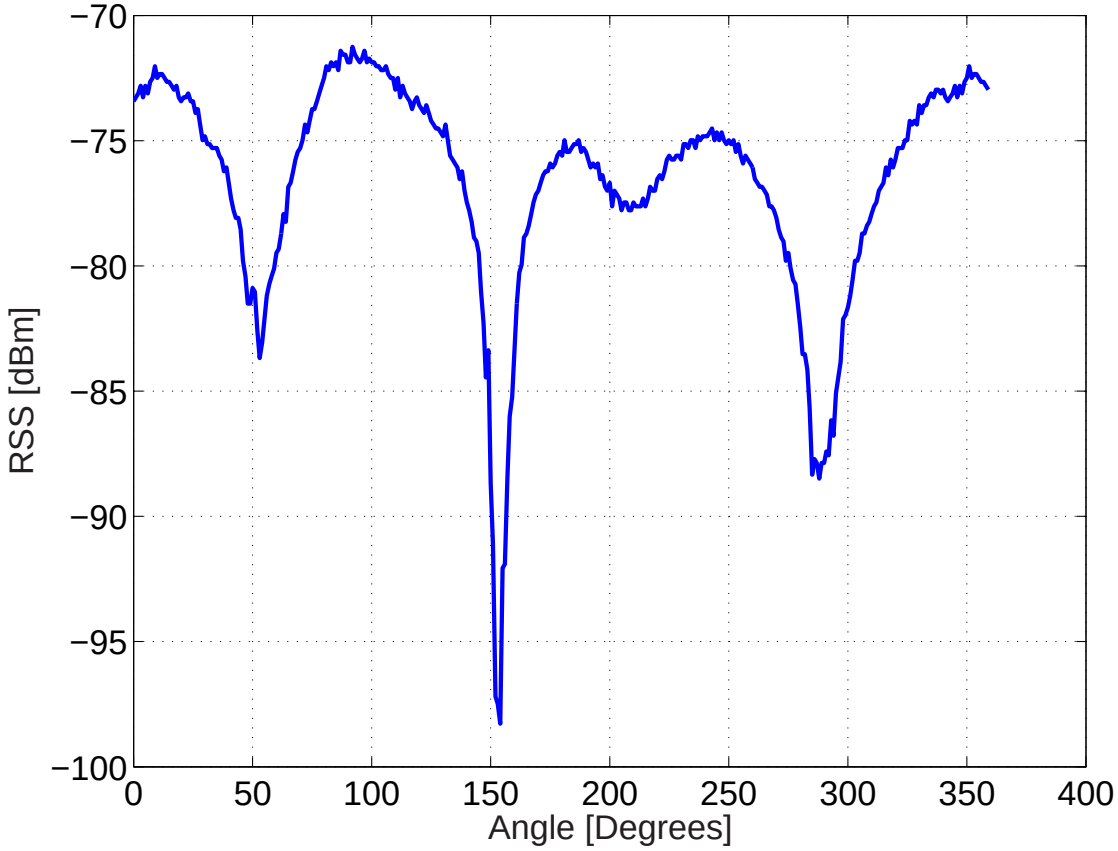

Figure 5.2. The oversampled channel such that a sample is taken every 1°

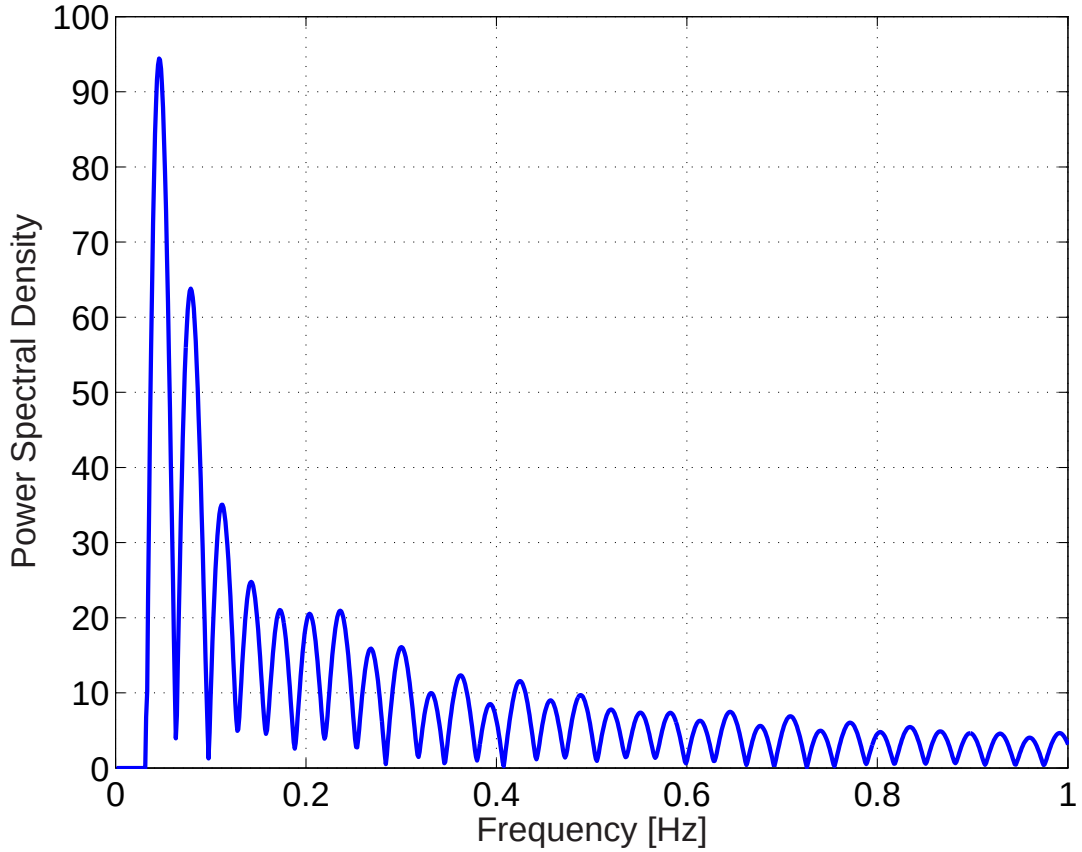

Figure 5.3. Power spectral density of the sampled channel.

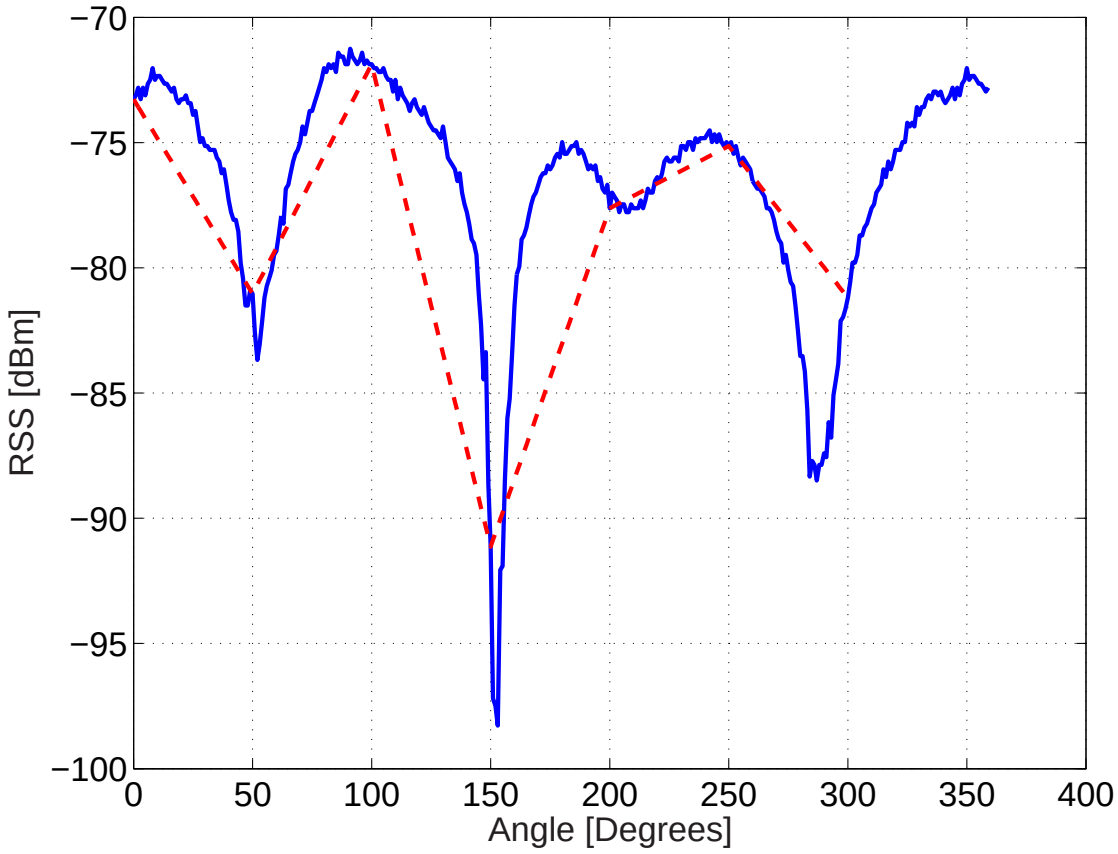

Figure 5.4. The downsampled channel, dashed line, superimposed on the oversampled channel, solid line.

degree, but it was not suitable to locate the position with the maximum RSS. In Figure 5.5, the channel was downsampled by 30 such that the distance between each sampled point was 9.68cm and then reconstructed with Nyquist interpolation technique. The maximum peak was very sensitive to the actual location of the samples taken, and the location of the resulting max peak varied greatly. In many of the interpolation tests, the location of the maximum peak was missed entirely such that one of the minor peaks was interpreted to have the maximum RSS.

The leakage effect is probably greatly responsible for the failure of the Nyquist interpolation in this experiment [26]. Only one period of the waveform was sampled since only one full revolution was conducted by the turntable. This created a very small sampling window for the Nyquist interpolation which is designed for an infinitely long stationary wave. However, it would be impractical to conduct more revolutions for the purpose of further sampling. The extra revolutions would consume even more time and energy and should be avoided if possible. It would be more practical to do one slow revolution and just oversample the channel.

The Nyquist reconstruction was also compromised by the overshooting resulting from the samples in the deep fades. Since the deep fades could occur abruptly, the Nqyuist reconstruction would compensate by overshooting and creating large peaks where they do not actually exist. One solution to handling this issue is to apply a low-pass filter with a cut-off frequency small enough to eliminate the deep fades from consideration in the Nyquist reconstruction. To test the feasibility of applying a LPF to the sampled channel, a low-pass first-order Butterworth filter with a small cut-off frequency was applied to the oversampled channel. The result can be seen in Figure 5.6.

Several issues are apparent from the result in Figure 5.6. The first issue is

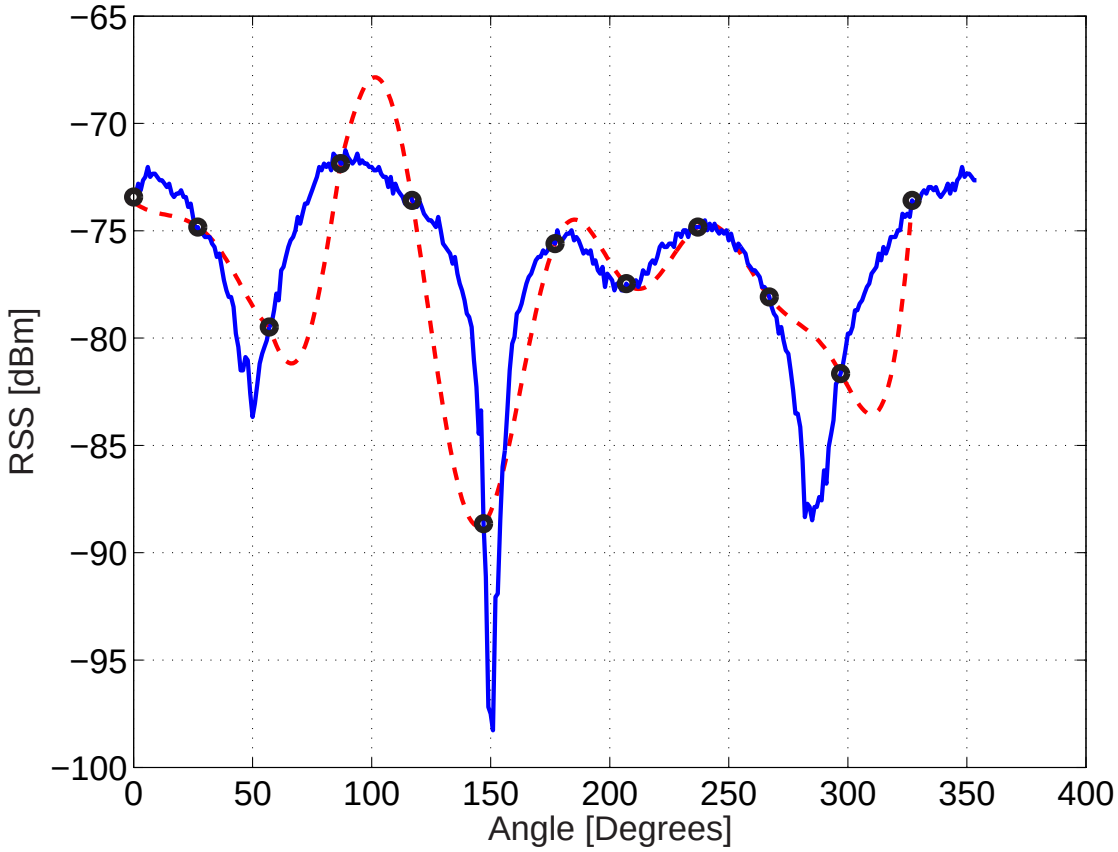

Figure 5.5. Reconstructed channel via Nyquist interpolation, dashed line, superimposed over the oversampled channel, solid line. The circled points are the points used for the Nyquist Interpolation.

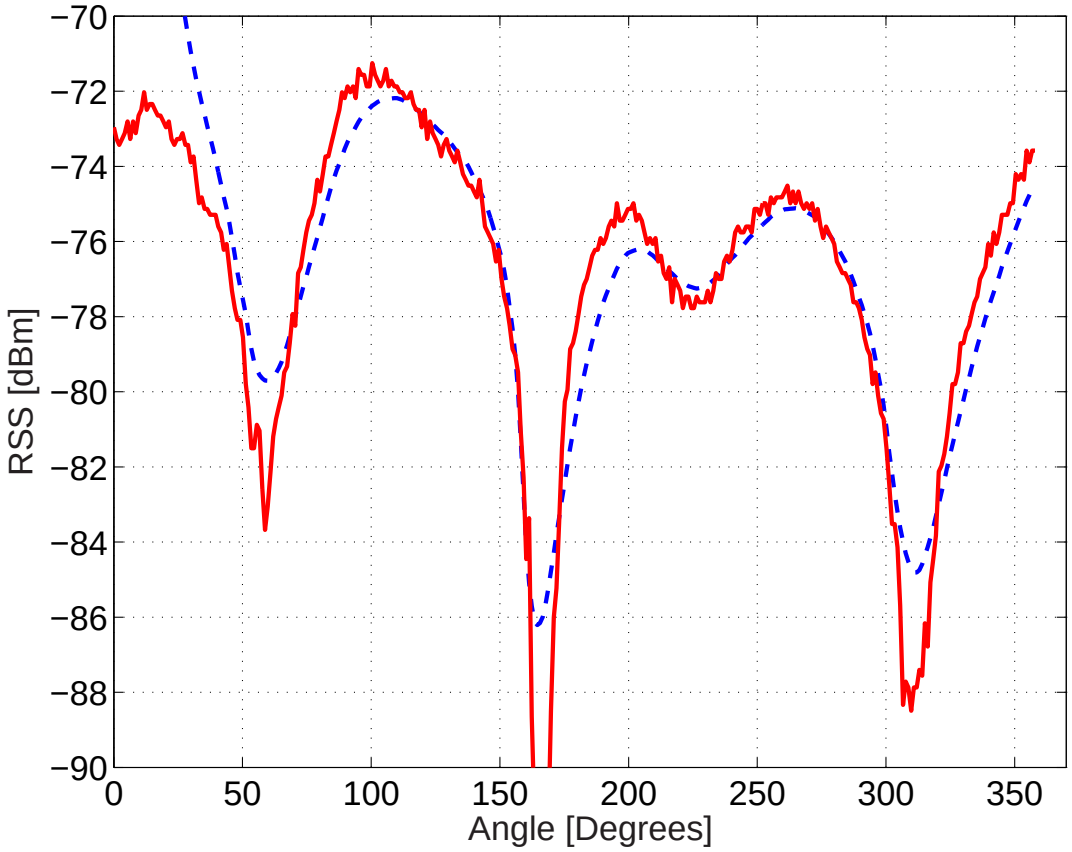

Figure 5.6. Result of applying the first-order Butterworth LPF where the solid line is the original oversampled channel while the dashed line is the channel after applying the LPF.

that the early set of samples, 0° to 40°, are too large and must be discarded. The LPF corrupts the first set of samples in the channel since there are no earlier set of samples to compensate for the effects of the LPF. Higher order filters increase the size of this range so a first-order filter was determined to the be the optimum choice since it has the smallest range of corrupted samples. The deep fade valleys from the result using the LPF in Figure 5.6 are less noticeable than the original channel. Although the LPF makes the deep fades less noticeable, it also affects the waveform and can affect the location of the maximum link quality. Also, the delay introduced by the LPF needs to be considered. Therefore, it appears that the LPF can be used in making the Nyquist reconstruction a more viable option, but a lot of effort is needed in properly designing the LPF so that it does not change the sampled channel so much such that the location of greatest link quality is shifted from the original location.

The results of the successful interpolation techniques can be seen in Table 5.1. Each of the values measured is the distance in centimeters that they are separated from the oversampled case. Therefore, if the interpolation is successful, the interpolation error distance should shrink from the original value.

As the distance between sampled points was increased, so did the error distance between the measured point and oversampled point. The cubic spline interpolation had mixed results. There were occasions such as when the points were 19.0cm apart, the cubic spline greatly lowered the error distance. However, there were other scenarios where it actually increased the error distance instead such as the 14.4cm/sample case. Consequently, the cubic spine performance is quite random in that it is effective when is operating properly, but there is a possibility that it will actually be detrimental to the performance of the COLMO node.

TABLE 5.1

SAMPLING AND INTERPOLATION PERFORMANCE

Sample Intervals (cm)	Wavelength	None (cm)	Cubic (cm)	3-Point (cm)
4.84	$\sim \lambda/14$	1.40	1.26	1.12
9.64	$\sim \lambda/7$	2.61	1.65	2.40
14.4	$\sim \lambda/5$	3.73	4.44	3.56
19.0	$\sim \lambda/4$	5.08	3.12	4.86
23.5	$\sim \lambda/3$	24.43	25.33	24.38

The 3-Point Interpolation technique proved to be consistently effective. While there are examples where it was not effective as the cubic spine case, there are no examples where it actually increased the error distance. It managed to always lower the error distance by 0.20cm. Also, it may be possible that the performance of this interpolation can be improved by modifying certain parts of its formula such as giving extra emphasis to larger slopes.

Once the channel becomes too downsampled, it exceeds a critical threshold where the distance error increases drastically. In this case, once the channel was downsampled to the point of 23.5cm, or approximately $\lambda/3$, the probability that the sampled position associated with the max RSS was even going to be found was 64%. In these instances, the interpolation became ineffective and could not lower the error distance by a noticeable degree.

In this test, the result from the Fourier transform was able to successfully predict the minimum sampling frequency. It predicted that the maximum allowable

distance between samples was 20.3cm, and the critical threshold was found to be between 19.0cm and 23.5cm. However, it was not simple in determining the location of the maximum allowable sampling frequency. As seen in Figure 5.3, there is little difference between the significant portion of the signal and the unneeded portion of the signal found after 0.425Hz. However, even this weak portion of the signal was vital in determining the sampling rate. Future models that use the FFT to determine of the properties of the channel need to take this detail into account.

CHAPTER 6

CONCLUDING REMARKS

WSNs share many issues with other ad hoc networks while having several unique issues of their own. Critical nodes, multipath, hidden nodes, and limited energy force WSNs to find distinctive solutions such as limited controlled mobility.

In Chapter 2, we explored how small movements of the mote can greatly affect the RSS although the change in distance between the two motes was minute. Movements larger than more than several wavelengths would have been required to handle problems such as shadowing; however, the small scale fading from multipath could be mitigated with controlled movements of a fraction of a wavelength. This form of spatial diversity was proven to improve the RSS. This solution is not computationally demanding even for the motes used in WSNs. These motes usually have limited computational ability and may not have the luxury of several powerful yet mathematically demanding coding schemes.

The diversity gain achieved through controlled limited mobility varied from channel to channel. The amount of improvement in the RSS from the mean RSS measured in the channel depended on how much variation in the channel was present. Therefore, mobile nodes with channels demonstrating Rayleigh fading usually displayed greater improvements than the channels showing Ricean Fading. The mobile platform is best used in environments where a LOS between the two motes is lacking.

The performance of COLMO nodes in networks was analyzed in Chapter 3. While Chapter 2 explores the link quality between two motes, Chapter 3 determines how the COLMO node can handle network issues. It was found that different positions for the COLMO sink was favorable for one set of notes while another position was favorable for another set. This property allowed the mobile BS to increase its choice of critical nodes, thus extending the lifetime of the network. When one set of critical nodes start to display low energy, the BS can move to another position and find another set of fresh nodes to take up the responsibility of handling the network traffic. The capability for limited mobility may give rise to new routing protocols and metrics that will consider how to best benefit from this ability.

The benefits of the limited mobility can be scaled to benefit even large networks consisting of thousands of nodes by applying COLMO relays. By adding mobility to the nodes serving as bottlenecks in the network, the overall efficiency of the network can be improved greatly. Sometimes nodes serve as poor relays due to the severe multipath fading and the option for limited mobility may make these nodes a practical choice to relay packets onward through the network. This will open new path for the network which were previously unavailable. While strategies such as [11] have been proposed to utilize the Rayleigh fading found in the network, the COLMO node may be able to enhance some of these techniques.

Chapter 4 determined which metric was the most effective in determining the link quality of a channel between two motes. Two common and popular options are the RSSI and the LQI. The LQI was proven to be a good indicator of the quality of poor and mediocre links. It could fairly accurately predict the probability that a packet will be dropped when it is transmitted across that link. The downside is

that the LQI needs to use a large averaging sampling window ranging up to 100 samples to give an accurate prediction. This extra latency may make the mobile node less effective if the link quality is constantly and rapidly changing. The second option, the RSSI, could quickly determine the RSS of the channel with one or several samples. While it can not predict the quality of weak channels, it does serve well in predicting the robustness of high quality channels. For example, two channels may both have nearly zero probability of packets being dropped, but the RSSI can determine which of these two channels will be the most robust against changes in the environment.

The final chapter, Chapter 5, studied the issues of sampling rates and interpolation. The sampled channel could be more quickly sampled if it needed to sample less positions. Therefore, the penalty of oversampling the spatial channel is extra latency. Conversely, the penalty for undersampling the spatial channel could be worse since the effectiveness of the COLMO node was jeopardized.

Several interpolation techniques were explored for scenarios where the channel was not too greatly oversampled. While the cubic spline interpolation proved to accurately curve trace the samples, there were examples where it predicted to position with the maximum RSS to be even farther away from the true position. Therefore, the 3-Point Interpolation proved to be a better option since it would be more likely to correctly determine the direction of the position with the max RSS from the point that was sampled with the max RSS.

Overall, the COLMO node appears to be a viable option in handling channels plagued with many positions of poor link quality resulting from small scale fading from multipath. Future work and analysis may find additional observations and techniques to increase its overall efficiency. This concept has the potential to serve

as a practical tool in future WSNs.

APPENDIX A

APPENDIX

A.1 Mobile Platforms Overview

There are several possible platforms that would viable for conducting a COLMO node experiment. They have to adhere to several conditions to be a successful mobile platform. One such important criteria is that the platform holding the mote is able to move the mote to many different locations that are separated far enough such that the correlation of the link quality between each position is weak. However, the platform must also be able to ensure that the distance between each position is small enough that the link quality within this distance can be predicted via interpolation. If the distance is too large for interpolation to be successful, the performance of the mote is jeopardized.

Since we are considering primarily WSNs, there are also several other conditions that should be considered. Since many COLMO nodes may be present in a large WSN, it ideal that the mobile platforms are as inexpensive as possible. They should be cheap so that they are not considered impractical in networks spanning several thousand nodes.

However, the mobile platform must be constructed so that it can perform very well within several specifications. It must be able to return to a previously sampled location with enough accuracy to satisfy the mote. The placement error,

the distance between the desired position and the actual position the platform found, needs to be small enough that the correlation between these two positions is very strong. Therefore, a placement error of a few millimeters may not affect most systems while a placement error of several decimeters may noticeable and severe. Generally, it is preferred that the placement error is less then $\lambda/20$. This means that motes that use high carrier frequencies such as the MicaZs with 2.4GHz will be more sensitive to the size of the placement error since they have a wavelength of 12.5cm.

A.2 Physical Design of the Experimental Turntable

An example of a mobile platform would be to use a mobile robot that could move throughout a specified range in the environment. However, the wide range of freedom may be impractical, and the robot platform could prove to be too costly to be economical. For the experiments performed in this thesis, I constructed a turntable with a circular platform with a radius of 29cm that could do complete revolutions clockwise and counterclockwise. This allowed the mote to travel in two dimensional space in a path defined by the perimeter of the circle with a radius of 29cm or less. If I wanted the mote to travel through less distance per a complete revolution, I placed the mote closer to the center of the turntable. This was a practical solution for the MicaZs which has a high carrier frequency. To obtain better results for the Mica2s, I found it practical to place them on the edge of the turntable. The physical diagram of the turntable can be seen in Figure A.1.

The motor used to rotate the platform is the HT23-393 stepper motor. A stepper motor was chosen because it allows a high amount of precision since it moves in well defined steps, but it can also move continuously. Also, the size of this

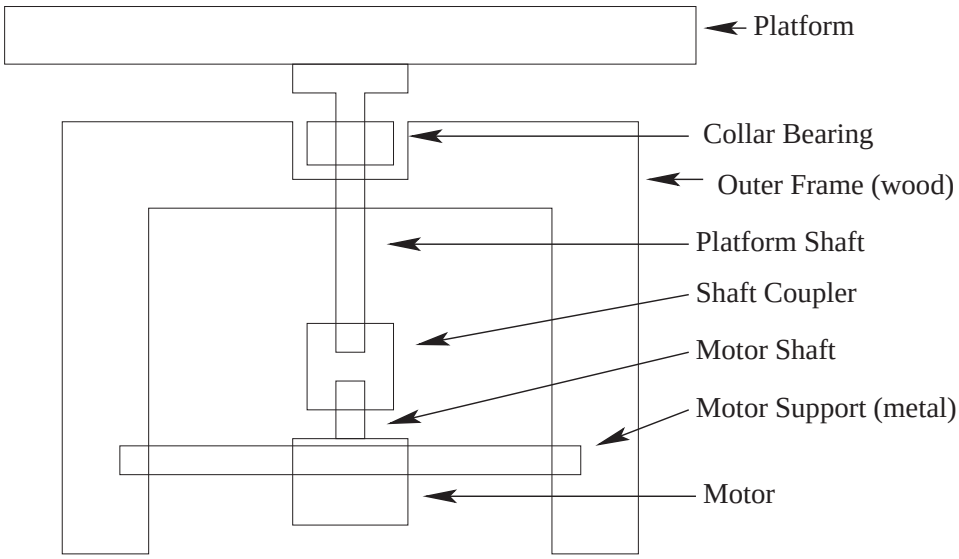

Figure A.1. Physical design of the turntable

motor is large enough that it has more than enough torque needed to easily move the platform without any concern for placement errors. It also has the ability to rotate clockwise and counterclockwise.

For simplicity, the rotating platform was constructed so that the motor shaft was directly coupled to the shaft of the turntable. This avoided additional structural complications that would have been present with the application of gears.

A.3 Communication between the Turntable And Motes

The MD2S-P-L from US Digital was used as the motor stepper driver that ensured that the stepper motor was driven correctly. The driver had one input port that used the frequency of a square wave to control the speed of the motor such that a higher frequency would result in the motor spinning faster. The second input would control the direction of the rotation of the motor such that a high

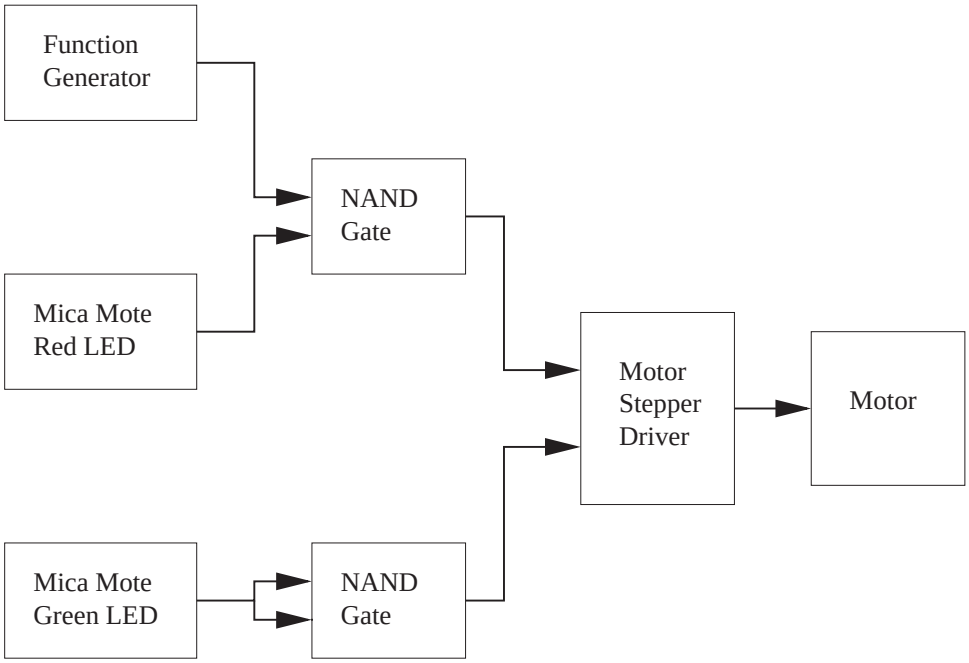

Figure A.2. Layout of the circuit driving the motor with a Mica mote.

input voltage would make the motor rotate clockwise while a low input voltage caused it to spin counterclockwise.

Figure A.2 shows how either Mica mote, Mica2 or MicaZ, was able to communicate properly with the stepper motor driver. The Mica motes both have a 51-pin socket where three pins are linked to their respective LED. So when the red LED goes from dark to illuminated, the voltage at the pin linked to that LED goes from 3 volts to 0 volts. The square wave is created by a function generator, and its frequency of its output controls the speed of the turntable.

The Mica mote allows or blocks the square wave signal from reaching the driver with the application of a NAND gate. When the red LED is on, the pin associated with that LED has its voltage drop to zero. This allows the square wave to pass through the NAND which in turn allows the motor to spin. For

intuitive simplicity, the pin linked to the green LED controls the direction and is inverted so that the turntable will turn clockwise when the green LED is on.

BIBLIOGRAPHY

1. "Self-healing Mines," http://www.darpa.mil/ato/programs/SHM/.

2. "Shooter Localization," http://www.isis.vanderbilt.edu/projects/nest/applications.html.

3. E. Biagioni and K. Bridges, "The app. of remote sensor technology to assist the recovery of rare and endangered species," *International Journal of High Performance Computing Applications*, vol. 16, no. 3, pp. 315–324, AUG 2002.

4. J. Burrell, T. Brooke, and R. Beckwith, "Vineyard Computing: Sensor Networks in Agricultural Production," *IEEE Pervasive Computing*, vol. 3, no. 1, pp. 38–45, 2004.

5. A. Cerpa, J. Wong, M. Potkonjak, and D. Estrin, "Temporal Properties of Low Power Wireless Links: Modeling and Implications on Multi-Hop Routing," in *"Proceedings of the 6th ACM international Symposium on Mobile Ad Hoc Networking and Computing"*, Urbana-Champaign, IL, USA, May 2005.

6. D. D. Couto, D. Aguayo, J. Bicket, and R. Morris, "A High-Throughput Path Metric for Multi-Hop Wireless Routing," in *Proceedings of the 9th Annual International Conference on Mobile Computing and Networking (MobiCom'03)*, San Diego, CA, USA, 2003.

7. Q. Dong, "Maximizing system lifetime in wireless sensor networks," in *IPSN '05: Proceedings of the 4th international symposium on Information processing in sensor networks*. Piscataway, NJ, USA: IEEE Press, 2005, p. 3.

8. R. Frenkiel, B. Badrinath, J. Borras, and R. Yates, "The Infostations Challenge: Balancing Cost and Ubiquity in Delivering Wireless Data," *IEEE Personal Communications*, vol. 7, no. 2, Apr 2000.

9. T. Fulford-Jones, D. Malan, M. Welsh, and S. Moulton, "CodeBlue: An Ad Hoc Sensor Network Infrastructure for Emergency Medical Care," in *International Workshop on Wearable and Implantable Body Sensor Networks*, London, UK, 2004.

10. A. Giorgetti, M. Chiani, M. Shafi, and P. J. Smith, "Level Crossing Rates and MIMO Capacity Fades: Impacts of Spatial/Temporal Channel Correlation," in *Communications, 2003. ICC '03. IEEE International Conference on*, vol. 5, May 2003, pp. 3046–3050.

11. M. Haenggi, "Energy-Balancing Strategies for Sensor Networks," *IEEE Transactions on Circuits and Systems*, 2005, submitted for publication. Available at http://www.nd.edu/~mhaenggi/pubs/tcas05.pdf.

12. ——, "On Routing in Random Rayleigh Fading Networks," *IEEE Transactions on Wireless Communications*, vol. 4, pp. 1553–1562, 2005.

13. ——, "A Geometry-Inclusive Fading Model for Random Wireless Networks," in *IEEE International Symposium on Information Theory (ISIT'06)*, Seattle, WA, USA, 2006.

14. ——, "Geometry, connectivity, and broadcast transport capacity of random networks with fading," in *2007 IEEE International Symposium on Information Theory (ISIT'07)*, vol. 43, Nice, France, June 2007.

15. M. Haenggi and D. Puccinelli, "Routing in ad hoc networks: A case for long hops," *IEEE Communications Magazine*, vol. 43, Oct 2005.

16. W. R. Heinzelman, A. Chandrakasan, and H. Balakrishnan, "Energy-efficient communication protocol for wireless microsensor networks," in *HICSS '00: Proceedings of the 33rd Hawaii International Conference on System Sciences-Volume 8*. Washington, DC, USA: IEEE Computer Society, 2000, p. 8020.

17. J. Hill and D. Culler, "Mica: A Wireless Platform for Deeply Embedded Networks," *IEEE Micro*, vol. 22, pp. 12–24, November 2002.

18. B. Holler and G. Oien, "On the Amount of Fading in MIMO Diversity Systems," *IEEE Transactions on Wireless Communications*, vol. 4, no. 5, Sep 2005.

19. T. Kijewski-Correa, M. Haenggi, and P. Antsaklis, "Wireless sensor networks for structural health monitoring: A multi-scale approach," in *17th Analysis and Computations Specialty Conference*, May 2006.

20. D. Lal, A. Manjeshwar, F. Herrmann, E. Uysal-Biyikoglu, and A. Keshavarzian, "Measurement and Characterization of Link Quality Metrics in Energy Constrained Wireless Sensor Networks," in *Proceedings of the IEEE 2003 Global Communications Conference (GLOBECOM'03)*, San Francisco, CA, USA, Dec. 2003, pp. 446–452.

21. R. Madan, S. Cui, S. Lall, A. Goldsmith, and S. Wicker, "Cross-layer design for lifetime maximization in interference-limited wireless sensor networks ," in *The 24th Annual Joint Conference of the IEEE Computer and Communications Societies (INFOCOM'05)*, Miami, FL, USA, Mar. 2005.

22. A. V. Oppenheim and R. W. Schafer, *Discrete-Time Signal Processing.* Prentice Hall, 1998.

23. R. Peng, S. Mao-heng, and Z. You-min, "ZigBee Routing Selection Strategy Based on Data Services and Energy-Balanced ZigBee Routing," in *Proceedings of the 2006 IEEE Asia-Pacific Conference on Services Computing*, Guangzhou, Guangdong, China, 2006.

24. C. Perkins and E. Royer, "Ad hoc On-Demand Distance Vector Routing," in *Proceedings of the 2nd IEEE Workshop on Mobile Computing Systems and Applications*, New Orleans, LA, USA, Feb. 1999.

25. J. Polastre, J. Hui, P. Levis, J. Zhao, D. Culler, S. Shenker, and I. Stoica, "A unifying link abstraction for wireless sensor networks," in *SenSys '05: Proceedings of the 3rd international conference on Embedded networked sensor systems.* New York, NY, USA: ACM Press, 2005, pp. 76–89.

26. J. G. Proakis and D. K. Manolakis, *Digital Signal Processing.* Prentice Hall, 2006.

27. D. Puccinelli and M. Haenggi, "Wireless Sensor Networks-Applications and Challenges of Ubiquitous Sensing," *IEEE Circuits and Systems Magazine*, vol. 5, p. 19, 2005.

28. ——, "Multipath Fading in Wireless Sensor Networks: Measurements and Interpretation," in *International Wireless Communications and Mobile Computing Conference (IWCMC'06)*, Vancouver, BC, Canada, July 2006.

29. ——, "Spatial Diversity Benefits by Means of Induced Fading," in *Third IEEE International Conference on Sensor and Ad Hoc Communications and Networks (SECON'06)*, Reston, VA, USA, 2006.

30. R. Rao, S. Vrudhula, and D. Rakhmatov, "Battery Modeling for Energy-Aware System Design," *IEEE Computer*, vol. 36, no. 12, dec 2003.

31. D. Reed, J. Smith, A. Rodriguez, and G. Calcev, "Spatial Channel Models for Multi-antenna Systems," in *Vehicular Technology Conference, 2003. VTC 2003-Fall. 2003 IEEE 58th*, vol. 5, Oct 2003, pp. 99–103.

32. C. Schurgers and M. Srivastava, "Energy Efficient Routing in Wireless Sensor Networks," in *MILCOM'01*, Vienna, VA, USA, Oct. 2001.

33. R. Shah and J. Rabaey, "Energy aware routing for low energy ad hoc sensor networks," in *IEEE Wireless Communications and Networking Conference (WCNC'02)*, Orlando, FL, USA, Mar 2002.

34. R. C. Shah, S. Roy, S. Jain, and W. Brunette, "Data MULEs: Modeling and analysis of a three-tier architecture for sparse sensor networks," in *Ad Hoc Networks Journal*, vol. 1. Elsevier, Sep 2003, pp. 215–233.

35. E. Shih, P. Bahl, and M. Sinclair, "Wake on Wireless: an Event Driven Energy Saving Strategy for Battery Operated Devices," in *Proceedings of the 8th Annual International Conference on Mobile Computing and Networking (MobiCom'02)*, Atlanta, GA, Sept. 2002.

36. K. Sohrabi, J. Gao, V. Ailawadhi, and G. Pottie, "Protocols for self-organization of a wireless sensor network," *IEEE Personal Communications Magazine*, vol. 7, no. 5, pp. 16–27, Oct. 2000.

37. K. Srinivasan and P. Levis, "RSSI is Under Appreciated," in *Third Workshop on Embedded Networked Sensors (EmNets'06)*, Cambridge, MA, USA, May 2006.

38. L. Tong, Q. Zhao, and S. Adireddy, "Sensor Networks with Mobile Agents," in *Proceedings of the IEEE Military Communications Conference*, Boston, MA, USA, 2003.

39. D. Tse and P. Viswanath, *Fundamentals of Wireless Communication*. Cambridge University Press, 2005.

40. P. Venkitasubramaniam, S. Adireddy, and L. Tong, "Sensor Networks with Mobile Access: Optimal Random Access and Coding," *IEEE Journal on Selected Areas in Communications*, vol. 22, no. 6, pp. 1058–1068, August 2004.

41. P. Venkitasubramaniam, Q. Zhao, and L. Tong, "Sensor network with multiple mobile access points," in *In Proc. Conf. on Info. Systems and Sciences*, Princeton, NJ, Mar. 2004.

42. W. Wang, V. Srinivasan, and K. Chua, "Using Mobile Relays to Prolong the Lifetime of Wireless Sensor Networks," in *Proceedings of the 11th Annual International Conference on Mobile Computing and Networking (MobiCom'05)*, Cologne, Germany, 2004.

43. A. Woo, T. Tong, and D. Culler, "Taming the Underlying Challenges of Reliable Multihop Routing in Sensor Networks," in *Proceedings of the 1st International Conference on Embedded Networked Sensor Systems (SenSys'03)*, Los Angeles, CA, USA, Nov. 2002.

44. K. Woyach, D. Puccinelli, and M. Haenggi, "Sensorless Sensing in Wireless Networks: Implementation and Measurements," in *Second International Workshop on Wireless Network Measurement (WinMee'06)*, Boston, MA, USA, Apr. 2006.

45. W. Zhao, M. Ammar, and E. Zegura, "A message ferrying approach for data delivery in sparse mobile ad hoc networks," in *The Fifth ACM International Symposium on Mobile Ad Hoc Networking and Computing (MobiHoc'04)*, Tokyo, Japan, May 2004.

46. W. Zhao and M. H. Ammar, "Message ferrying: Proactive routing in highly-partitioned wireless ad hoc networks," in *FTDCS '03: Proceedings of the The Ninth IEEE Workshop on Future Trends of Distributed Computing Systems (FTDCS'03)*. Washington, DC, USA: IEEE Computer Society, 2003, p. 308.

47. S. Zhou, R. Liu, and J. Guo, "Energy Efficient Networking Protocols for Wireless Sensor Networks," in *IEEE Conference on Industrial Informatics (INDIN'06)*, Aug. 2006.

48. M. Zuniga and B. Krishnamachari, "Analyzing the Transitional Region in Low Power Wireless Links," in *Proceedings of the First IEEE International Conference on Sensor and Ad hoc Communications and Networks (SECON'04)*, Santa Clara, CA, USA, Oct. 2004.

This document was prepared & typeset with LaTeX 2ε*, and formatted with* NDdiss2ε *classfile (v3.0[2005/07/27]) provided by Sameer Vijay.*